Biosensors and Bioelectronics 185 (2021) 113242

Contents lists available at ScienceDirect

Biosensors and Bioelectronics

journal homepage: http://www.elsevier.com/locate/bios

Biomimetic electrochemical sensors: New horizons and challenges in biosensing applications

Pedro V.V. Romanholo [a], Claudia A. Razzino [b], Paulo A. Raymundo-Pereira [c], Thiago M. Prado [d], Sergio A.S. Machado [d], Livia F. Sgobbi [a,*]

[a] Instituto de Química, Universidade Federal de Goiás, Goiânia, GO, 74690-900, Brazil
[b] Instituto de Pesquisa e Desenvolvimento, Universidade Do Vale Do Paraíba, São José Dos Campos, SP, 12244-000, Brazil
[c] Instituto de Física de São Carlos, Universidade de São Paulo, São Carlos, SP, 13566-690, Brazil
[d] Instituto de Química de São Carlos, Universidade de São Paulo, São Carlos, SP, 13566-590, Brazil

ARTICLE INFO

Keywords:
Biomimetic electrochemical sensors
Molecularly imprinted polymers
Synzymes
Nanozymes
Metal complexes
Nanochannels

ABSTRACT

The urge to meet the ever-growing needs of sensing technology has spurred research to look for new alternatives to traditional analytical methods. In this scenario, the glucometer is the flagship of commercial electrochemical sensing platforms, combining selectivity, reliability and portability. However, other types of enzyme-based biosensors seldom achieve the market, in spite of the large and increasing number of publications. The reasons behind their commercial limitations concern enzyme denaturation, and the high costs associated with procedures for their extraction and purification. In this sense, biomimetic materials that seek to imitate the desired properties of natural enzymes and biological systems have come out as an appealing path for robust and sensitive electrochemical biosensors. We herein portray the historical background of these biomimicking materials, covering from their beginnings until the most impactful applications in the field of electrochemical sensing platforms. Throughout the discussion, we present and critically appraise the major benefits and the most significant drawbacks offered by the bioinspired systems categorized as Nanozymes, Synzymes, Molecularly Imprinted Polymers (MIPs), Nanochannels, and Metal Complexes. Innovative strategies of fabrication and challenging applications are further reviewed and evaluated. In the end, we ponder over the prospects of this emerging field, assessing the most critical issues that shall be faced in the coming decade.

1. Introduction

Electrochemical biosensors have emerged as a promising analytical tool for *in situ* and real time detection in a myriad of applications (Arduini et al., 2016; Cho et al., 2020; El Harrad et al., 2018; Kurbanoglu et al., 2017; Majdinasab et al., 2017; Uniyal and Sharma 2018). Those devices are conducive to miniaturization and provide fast response, which are strict requirements for point-of-care (POC) technologies (Mohan et al., 2020; Silveira et al., 2016; Soleymani and Li 2017). Electrochemical biosensors also associate the sensitivity of electrochemical transducers with the high specificity and selectivity of biological recognition elements (i.e. enzymes, nucleic acids, antibodies, etc). They harness all these exquisite assets to deliver analytical measurements with simple and user-friendly formats.

Electrochemical-based devices currently dominate the biosensors market, which is projected to grow at a compound annual growth rate of 7.4% between 2021 and 2027 (Ugalmugle and Swain 2021). Diagnosis and health monitoring applications drive the market of electrochemical biosensors, particularly towards the thriving demand for POC testing (Pereira da Silva Neves et al., 2018). The largest market share of electrochemical systems is pushed by the cost-effective and scalable technology majorly owned by screen printed electrodes used on the POC strips (Dedeoglu et al., 2020).

Regarding commercial purposes, attributes such as versatility, miniaturization, reliability and device cost are imperative. Various technical issues must be considered for the market, concerning robustness, reliable and fast response, and prevention of sensor fouling (Bahadır and Sezgintürk 2015; Liu et al., 2019b; Monteiro and Almeida 2019). Additionally, the approval of regulatory agencies by means of comparison with standardized analytical protocols is mandatory (Mazzocchi 2016).

Aside from the glucometer, most biosensors are unable to accomplish

* Corresponding author.
E-mail address: livia_sgobbi@ufg.br (L.F. Sgobbi).

https://doi.org/10.1016/j.bios.2021.113242
Received 15 January 2021; Received in revised form 5 April 2021; Accepted 7 April 2021
Available online 17 April 2021

those conditions, mainly owing to limitations of the biological recognition element (Dedeoglu et al., 2020; Monteiro and Almeida 2019; Pereira da Silva Neves et al., 2018). Testing strips for the self-monitoring of blood glucose held nearly 77% of the worldwide biosensor market in 2019 (Ugalmugle and Swain 2020), since glucose oxidase (GOx) is relatively low-cost, with appropriate stability for immobilization (Gibson 1999; Raba and Mottola 1995; Tello et al., 2016). GOx is particularly stable when stored within a relatively wide interval of temperatures (5–40 °C) which is crucial for commercial strips (Tello et al., 2016). Although specific attributes regarding the high storage stability of commercially available glucometers are protected by patents, the capillary chamber where the enzyme is retained along with mediators and stabilizers seems to play a major role in it (Tello et al., 2016). Despite the commercial success of the glucometer, some challenges still persist for applications that rely on stability for long term usage since most strips can be stored for no more than two years under ideal conditions (van Enter and von Hauff 2018).

There is a plethora of publications and patenting activities related to the development of electrochemical biosensors for the detection of environmental pollutants, food contaminants and biomarkers, but they rarely achieve commercialization (Antonacci et al., 2016; Scognamiglio et al., 2010). Most of biosensing assays have been performed under controlled conditions and evaluated using buffer solutions considered as "fairly clean" samples rather than complex real-world samples (Dedeoglu et al., 2020; Luong et al., 2008; Luque de Castro and Herrera 2003). Particularly, it may alert that methods based on enzymatic inhibition can lead to false positive outcomes, since several compounds inhibit enzyme activity, decreasing sensor selectivity and affecting its sensitivity (Dhull et al., 2013; Luque de Castro and Herrera, 2003; Songa and Okonkwo 2016).

The development of commercially viable biosensors has been highly challenging regarding the limitations correlated with natural enzymes. The main drawbacks include incompatibility with organic solvents, limited stability, high cost associated with demanding extraction and purification processes, and restricted experimental conditions of pH, temperature, and ionic strength (Gibson 1999; Kuah et al., 2016; Reyes-De-Corcuera et al., 2018). The major concern hindering most electrochemical biosensors commercialization is related with the lack of robustness and reliability of those devices due to the low long-term activity, reproducibility and matrix interference (Pereira da Silva Neves et al., 2018; Scognamiglio et al., 2010; Silveira et al., 2016). Another pivotal matter regards the enzyme immobilization. Once immobilized on the electrode surface, enzymes undergo conformational changes resulting in activity loss which affects the biosensor sensitivity and its short-term storage (Tello et al., 2016). These issues still remain unsolved and demand additional efforts.

In order to overcome the aforementioned drawbacks attributed to the biological recognition element, artificial enzymes and molecularly imprinted polymers have been developed to mimic enzymatic performance or to promote specific binding affinity towards target analytes (Arduini et al., 2017; Lowdon et al., 2020b; Scognamiglio et al., 2015; Sezgintürk 2020; van Enter and von Hauff 2018; Yang et al., 2016a). These elements offer outstanding possibilities in the developments of new electrochemical sensors, designated as biomimetic ones. Non-enzymatic biosensors based on biomimetic materials are focus of intense research since they offer the possibility of overcoming the recurrent stability issues, paving the way for the mass production and commercialization of viable sensors (Hwang et al., 2018; Yang et al., 2016a). Furthermore, the progress in material science and microengineering has boosted the development of wearable, easy-to-use, low-cost, and noninvasive biosensors. However, they are mostly used for research purposes, and the integration of biomimetic materials with commercial devices is still under progress.

Herein, we explore the potentialities of biomimetic materials as a promising trend in sensing technologies. This review covers the state-of-the art of Biomimetic Chemistry, including the main types of biomimetic materials (nanozymes, molecularly imprinted polymers, synzymes, metal complexes, and nanochannels), their properties and integration with electrochemical platforms, comparing their activity with those of native enzymes. Additionally, we highlight current challenges behind biomimetic electrochemical sensors, possible solutions and pathways to address these limitations. To the best of our knowledge, no review paper is currently available combining the main types of biomimetic materials and their integration in electrochemical sensing platforms. There are, however, several reviews focusing on some of those aforementioned biomimetic materials alone, for instance, nanozymes. Those papers discuss their synthesis and function (Singh 2019; Zhou et al., 2017), their application in biosensing, immunoassays, cancer diagnostics and therapy, and pollutant removal (Jiang et al., 2019; Liang and Yan 2019; Wei and Wang 2013; Wu et al., 2019b). Nevertheless, the focus given in biosensing application is centralized in colorimetric/fluorimetric transducing, while electrochemical ones are briefly explored due to the predominance of the former systems (Huang et al., 2019a; Shin et al., 2015). Only recently, Mahmudunnabi et al. (2020) discussed more deeply about nanozyme-based electrochemical biosensors focusing solely on disease biomarkers applications; and Campuzano et al. (2020) covered recent advances in nanozyme-based electrochemical affinity biosensors. Concerning synzymes and metal complexes, there are no reviews covering these topics as biomimetic materials and their applications in electrochemical sensing. Our endeavor is to broaden the horizons in Biomimetic Chemistry as an auspicious direction in electrochemical biosensing.

2. Biomimetic Chemistry

Biomimetic Chemistry is a term coined by Prof. Ronald Breslow as the branch of organic chemistry which seeks to imitate natural reactions and enzymatic processes concerning the achievement of useful synthetic pathways (Breslow 1972, 1982, 1995). The attempt to imitate biological processes covers a wide range of themes, comprising artificial enzymes (Marchetti and Levine 2011); affinity-based systems (Chen et al., 2016a); self-assembly of small molecules analogous to biological membranes (He et al., 2009); and generation/redesign of novel biological system based on synthetic biology (Andrianantoandro et al., 2006).

Even though the evolutionary development of enzymes has led to their incomparable catalytic performance, their structure is easily affected by environmental stress, for instance temperature, pH, salt concentration, and even the presence of other enzymes. The aforementioned factors significantly hinder the application of enzymes in industry, where reaction environments are not as carefully controlled as those of biological systems (Nothling et al., 2019). A long-lasting challenge in Biomimetic Chemistry has been to reach simple synthetic systems capable of mimicking enzymes to overcome the operating window limitations of natural enzymes (Dong et al., 2012).

The motivation behind mimicking enzymatic reactions not only regards the velocity of the catalyzed processes, but also the accomplishment of high selectivity, both outstanding features of enzyme-catalyzed reactions (Breslow 1972, 1980).

Artificial enzymes can be designed mimicking the structure of a natural enzymes (e.g. active site) or enzyme functions (catalytic performance) (Raynal et al. 2014a, 2014b). Enzymes commonly bind their substrates, and thereupon use a few functional groups to perform catalysis. In aqueous media, binding can be achieved by metal or Lewis acid-base coordination or hydrophobic interaction. On the other hand, in nonaqueous solvents it happens through metal coordination, ion paring, Lewis acid-base coordination, or hydrogen bonding (Breslow 1995). The design of biomimetic models may take advantage of the aforementioned binding possibilities to create new systems.

Over the past few years, an assortment of materials have been employed as enzyme mimics, including supramolecular structures, polymers, nanoparticles, metallic complexes, etc (Marchetti and Levine 2011; Ndunda 2020; Raynal et al., 2014b; Rebilly et al., 2015; Wei and

Wang 2013; Wu et al., 2019b). They have been successfully applied to several fields, especially to chemical/biological sensing (Kuah et al., 2016). Over time, the development of Biomimetic Chemistry has been marked by several landmarks of material science closely related to the evolution of electrochemical sensing platforms (Fig. 1) from supramolecular structures to more recent approaches, such as multienzyme mimetic nanostructures. Thereby, the critical issues of some natural enzymes have been circumvented to achieve trustworthy electrochemical performances, ascribing robustness, reliability, sensitivity and stability in biosensing (Scognamiglio et al., 2015; Vial and Dumy 2009; Yang et al., 2016a). Generally, the keywords associated with those biosensors are "biomimetic", "non-enzymatic", "enzymeless", "enzyme-like" (e.g. peroxidase-like), "mimic", and "enzyme-free". In the following sections, we discuss the five main classes of biomimetic materials, starting with nanozymes.

3. Nanozymes – nanomaterials with catalytic activity

The past several years have witnessed an accelerated progress in enzyme-like catalytic nanomaterials (Wu et al., 2019b), widely disseminated as "nanozymes" since the first comprehensive review about this topic (Wei and Wang 2013). Advances in catalysis science, nanotechnology and computational design have boosted the imitation of new enzymes and the elucidation of their catalytic mechanisms, leading to a wide spectrum of applications (Huang et al., 2019b). Up to now, a number of excellent reviews have been published covering certain specific topics of nanozymes, such as biomedical applications (Jiang et al., 2019; Liang and Yan 2019; Wang et al., 2020b) biosensing and immunoassays (Niu et al., 2019; Wang et al., 2018a), food quality and safety detection (Huang et al., 2019a), environmental analysis (Li et al., 2019b), and general aspects of nanozymes (Singh 2019; Wu et al., 2019b; Zhou et al., 2017).

The development of nanozymes has been marked by several milestones. The first breakthrough was reported by Manea et al. (2004) who dubbed the self-assembly of triazacyclonane-functionalized thiols on the surface of nanosized gold nanoparticles upon complexation with Zn^{II} as a "nanozyme". This structure exhibited outstanding catalytic behavior for the cleavage of phosphate esters likewise ribonuclease (RNAse). Most RNAses require for their activity at least two metal ions that work cooperatively, particularly Zn^{II} ion is biologically relevant in phosphate-cleavage catalysis (Sträter et al., 1996). From this seminal result a new horizon has been opened up for new catalytic nanomaterials.

Thereupon, Comotti et al. (2004) reported that water-dispersed gold sol revealed a remarkable activity when used as "naked particles" (in the absence of common protectors) towards glucose oxidation. Their catalytic behavior was comparable to that of enzymatic systems, being one order of magnitude less active than the native enzyme. Under similar conditions, other metals were evaluated (e.g. Pt, Cu, Ag and Pd), but they did not exhibited any significant oxidase-mimic activity. Detailed mechanism studies suggested that glucose may be first adsorbed onto gold nanoparticles; and then oxygen reacts with the adsorbed glucose to form products (gluconic acid and H_2O_2) (Beltrame et al., 2006). Selectivity studies regarding the oxidation of other types of sugar were not performed. However, selective oxidation of D-glucose on colloidal gold catalyst was confirmed with no formation of side products (Biella et al. 2002a, 2002b). Gold nanoparticles are then a competitive alternative for glucose oxidation due to their simplicity of catalyst manufacturing, nontoxicity and possibility of recycling.

Another interesting nanoparticle is nanoceria which was demonstrated to act as an antioxidant owing to its ability to reversibly switch from Ce^{3+} to Ce^{4+} (Das et al., 2007). Later studies showed an intrinsic oxidase-like activity of nanoceria towards the oxidation of several organic substrates without any addition of an oxidizing agent, such as hydrogen peroxide (Asati et al., 2009). Thereby, the activity of nanoceria as oxidase instead of peroxidase was verified since no H_2O_2 was added in the system. The aforementioned catalytic behavior is not only pH-dependent but also dependent on the size and coating of cerium oxide nanoparticles. The superior performance was provided by smaller sized nanoparticles at acidic conditions and thinner coatings.

A further milestone in the nanozymes scenario was reported by Yan's Group (Gao et al., 2007) through the surprising discovery that Fe_3O_4 nanoparticles possess intrinsic peroxidase-like activity. They evaluated the catalytic performance of different sized Fe_3O_4 nanoparticles towards the oxidation of organic substrates (3,3,5,5-tetramethylbenzidine (TMB), di-azo-aminobenzene (DAB) and o-phenylenediamine (OPD)) in the presence of hydrogen peroxide. The smaller the particle size, the higher the catalytic activity likely due to a greater surface-to-volume ratio to interact with substrates. At the same molar concentrations, Fe_3O_4 showed a level of activity 40-fold higher than horseradish peroxidase (HRP). Probably, the presence of ferrous and ferric ions in the nanoparticles is fundamental to their catalysis, suggesting that Fe^{2+} ions may play a pivotal role in catalytic peroxidase-like activity.

In the last decade, a highlight in the field of nanozymes was the discovery of peroxidase-like activity of carbon-based materials by Qu's group, such as graphene oxide (GO) (Song et al., 2010a) and single walled carbon nanotubes (SWCNTs) (Song et al., 2010b). Both nanomaterials catalyzed the reaction of the peroxidase substrate TMB in the presence of H_2O_2 to produce a blue solution. Kinetic studies revealed that GO presented a higher catalytic activity towards TMB than the natural HRP. Further studies indicated that the peroxidase-like activity was an intrinsic property of both GO and SWCNT, not related to the trace

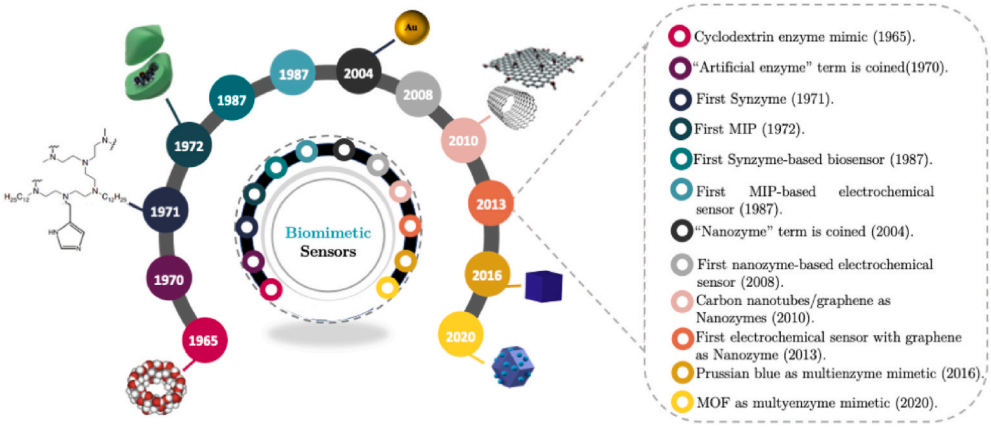

Fig. 1. A brief timeline for the evolution of biomimetic electrochemical sensors tied to the progress of artificial enzymes and MIPs (see Table S1, **ESI** for related references).

amount of metal catalyst in the sample. In comparison to HRP, GO is cost-effective, easy to obtain and more stable to biodegradation. GO and SWCNT-catalysis were strongly dependent on pH, temperature, and H_2O_2 concentration, similar to HRP. Recently, Wang et al. (2020a) investigated the possible catalytic mechanisms of graphene-based materials responsible for their peroxidase mimicking activities using DFT calculations. The oxidation of TMB in the presence of H_2O_2 was used as a model. The authors concluded that carbonyl groups are the catalytic active centers, whereas carboxyl groups are much less effective. Besides, ether is very stable and does not act as a catalytic center. Although epoxy, hydroxyl and endoperoxide are also not catalytic centers, they are able to react with TMB generating blue oxTMB.

Remarkably, certain nanomaterials can mimic two or more types of enzymes, enabling different applications (Alizadeh and Salimi 2021; Alizadeh et al., 2020; Guo and Guo 2019; Liu et al., 2020; Zhang et al., 2021; Zhao et al., 2018). For instance, CeO_2 nanoparticles can perform different enzymatic activities at different pH values, and their catalytic activity depends on the Ce^{3+} surface area concentration (Baldim et al., 2018; Xu et al., 2013a). At neutral or high pH conditions, CeO_2 behaves as superoxide dismutase (SOD) and catalase mimics, while at low pH values, it behaves as SOD, peroxidase and oxidase mimics (Alizadeh et al., 2020; Xu et al., 2013a). Amongst the multi-enzyme mimics, Prussian blue (PB) cubic nanoparticles are particularly interesting due to their biocompatible nature, biodegradability, ease to synthesize, controllable shape and morphology, low production cost and their remarkable electrochemical mediator properties (Matos-Peralta and Antuch 2019; Patra 2016). Zhang et al. (2016) first reported the multi-enzymatic mimetic activity of PB nanoparticles which could effectively scavenge reactive oxygen species towards peroxidase, catalase, and SOD activities. They theorized that the multi-enzymatic mimic activities of PB nanoparticles were likely caused by the abundant redox potentials of their different forms owing to their efficiency as electron transporters.

So far, nanozymes have held a prominent place among biomimetic materials applied to electrochemical sensors (Campuzano et al., 2020; Mahmudunnabi et al., 2020). These nanomaterials have brought diverse compelling attributes to be used in electrochemical sensing devices, such as low-cost synthetic routes, large-scale production, wide possibilities of chemical functionalization and large surface area (Jiang et al., 2019; Liu and Liu 2017). They may outperform natural enzymes due to their enhanced stability and robust catalytic performance over harsh experimental conditions (extreme pH and/or temperature, non-aqueous solvent and digestion from proteases) (Chatterjee et al., 2020; Liu 2019). All these qualities along with the optical, electrochemical and magnetic properties of specific types of nanozymes enable their integration into different analytical systems (Gayda et al., 2020).

3.1. Electrochemical sensors based on nanozymes

The first electrochemical sensor which applied a nanostructure mimicking a natural enzyme was reported by Zhang et al. (2008). The authors employed Fe_3O_4 nanoparticles (NPs) as a peroxidase mimic to electrocatalyze H_2O_2 reduction. They successfully obtained a low cost and robust sensor by immobilizing Fe_3O_4 NPs through a layer-by-layer approach to selective detect H_2O_2 over ascorbic acid (AA) and uric acid (UA). The enzymeless sensor showed a good sensitivity and enhanced stability since Fe_3O_4 NPs maintained their electrocatalytic performance even in high-temperature incubation. This breakthrough inspired the development of several enzymeless electrochemical sensors via finely tailored engineering involved in nanoparticles production.

Iron oxide nanoparticles, including Fe_3O_4 and Fe_2O_3, constitute one of the most typical nanozymes applied to electrochemical biosensing (Table 1). Generally, they exhibit peroxidase-like or catalase-like activities under physiological reaction conditions and follow Michaelis-Menten kinetics (Gao et al., 2017). These foregoing two natural enzymes contain a porphyrin heme cofactor in their active site, and while both use hydrogen peroxide as substrate, only peroxidase generates free radicals to react with a hydrogen donor, whereas catalase generates oxygen (Gao et al., 2017).

Studies have shown that the peroxidase-like activity emerges from the intact nanoparticles rather than free ions (Gao et al., 2007; Wei and Wang 2008). Thus, iron oxide nanozymes can be figured out as a heterogenous Fenton system, whose kinetic performance involves substrate binding, surface reaction and product release (Gao et al., 2017). Even though the enzymatic properties and related kinetics of iron oxide NPs are now well-established, their fundamental mechanisms remain unknown. In iron oxide NPs, Fe^{2+}/Fe^{3+} ions are probably confined and coordinated tetrahedrally or octahedrally allowing to achieve effective electron transfer, similarly as in heme groups in peroxidase/catalase enzymes. It is still cumbersome to confirm the accurate structure of active sites in iron oxide NPs due to the complex environment of iron (Gao et al., 2017). However, pieces of evidence indicate that the active sites are located on the surface. Therefore, surface functionalization may improve affinity and selectivity for substrates. For instance, Fan et al. (2017) demonstrated that the partial grafting of iron oxide NPs with imidazole groups has improved the affinity for H_2O_2 in both peroxidase and catalase activity.

After the pioneering work of Zhang et al. (2008), other nanozyme-based electrochemical biosensors have arisen (Table 1). Manifold nanomaterials have been used to mimic different classes of enzymes, such as peroxidases (Bhattacharjee et al., 2018; Das et al., 2019; Gallay et al., 2020; Kang et al., 2021; Li et al. 2019a, 2020, 2021; Savas and Altintas 2019), oxidases (Liu et al., 2019a; Su et al., 2018; Wei et al., 2021a), catalase (Koyappayil et al., 2020; Neal et al., 2017; Wang et al., 2019), and superoxide dismutase (SOD) (Cai et al., 2020; Zhao et al. 2019a, 2021; Zheng et al., 2019). Those enzyme-like nanostructures are able to perform the same reactions as their natural counterparts (Fig. 2).

Thereby, numerous sensing architectures have become conceivable since nanozymes can catalyze different substrates, and the analyte detection can proceed direct or indirectly. Indirect detection is particularly convenient for electrochemical sensing when the target is not electroactive. Generally, the strategies involving electrochemical transducing and nanozymes encompass label-based and label-free detection systems. Concerning these aforementioned approaches, nanozymes can be used as an electrode material for the analyte detection, or as a label for signal amplification. Nanozymes offer high surface area and high density of capture sites to enhance the loading of electroactive species at their surface increasing the electrochemical response (Mahmudunnabi et al., 2020). Accordingly, 2D nanomaterials (Savas and Altintas 2019; Singh et al., 2017; Tian et al., 2018b; Wu et al., 2021), and also metal organic frameworks (MOFs) (Li et al., 2020; Ling et al., 2020; Wei et al., 2021a) have shown exceptional performance as nanozymes in electrochemical sensors. Zhao et al. (2021) designed a SOD-like heterostructure assembling 2D $Mn_3(PO_4)_2$ nanosheets with biomimetic activity and 2D MXene nanosheets (Ti_3C_2Tx) with high conductivity and abundant functional groups to detect $O_2^{\bullet-}$ at a low limit of detection of 1.63 nM. Meanwhile, Kong et al. (2020) used Ag NPs/flake-like zinc MOF with peroxidase mimetic activity as a signal amplifier for the sensitive photoelectrochemical detection of bleomycin antibiotic with a limit of detection of 0.18 nM. The Ag NPs were uniformly deposited in MOFs, increasing the number of active sites and the catalytic activity. MOF-based nanozymes are an auspicious new class of nanozymes owing to their uniform cavities which are prone to yield biomimetic active centers and pseudo-substrate-binding pockets (Niu et al., 2020). MOF-based nanozymes exhibit versatile structures and functions, with benefits of relatively low cost, simple preparation and tailored design. A remarkable approach using MOF with multi-enzyme activity was reported by Liu et al. (2020) to detect 3,4-dihydroxyphenylacetic acid (DOPAC), a metabolite of the neurotransmitter dopamine, through a real-time online electrochemical system (Fig. 3A–a)). The authors synthesized a "raisin pudding"-type ZIF-67/$Cu_{0.76}Co_{2.24}O_4$

Table 1
Selected nanozyme-based electrochemical biosensor works.

Nanozyme	Pseudo-enzymatic activity	Substrate	Linear range	LOD	Sensor configuration	Target	Reference
Mesoporous Fe_2O_3	Peroxidase	TMB	–	10% of methylation	SPGE/Fe_2O_3-5mC	Global DNA methylation	Bhattacharjee et al. (2018)
Fe_3O_4NPs	Peroxidase	H_2O_2	100 μM- 1.8 mM	103 μM	FTO/Fe3O4@CTAB/PSS	H_2O_2	Guivar et al. (2015)
Fe_3O_4NPs	Peroxidase	4-chloro-1-naphthol	50 fg/mL to 1 ng mL^{-1}	18 fg/mL	ITO/ZnO-NRs/$ZnIn_2S_4$/CS/BSA/Ab1	Prostate-specific antigen (PSA) based on sandwich assay	Li et al. (2019a)
Fe_3O_4	Peroxidase	H_2O_2	$10^{-9} - 10^{-2}$M	0.1 nM	Au/Cys/GA/Fe_3O_4 NPs/ChOx	Choline chloride	Zhang et al. (2011a)
Fe_3O_4	Peroxidase	H_2O_2	0.2–2.0 mM	0.01 mM	ITO/APTES/Fe_3O_4 NPs	H_2O_2	Zhang et al. (2011b)
AuNPs	Peroxidase	TMB	$60.0 - 6.0 \times 10^7$ CFU mL^{-1}	60 CFU mL^{-1}	Bare SPE	*P. aeruginosa*	Das et al. (2019)
RGO/His@AuNCs	Oxidase	NO_2^-	2.5–5700 μM	0.7 μM	GCE/RGO/His@AuNCs	NO_2^-	Liu et al. (2019a)
AuNPs	Peroxidase	Thionine	0.1–60.0 nM	0.06 nM	Bare Au electrode	Kanamycin	Wang et al. (2016)
DNA/AgNCs	Peroxidase	H_2O_2	$10^{-10} - 10^{-5}$ M	42 pM	Au/S1/S2	Lysozyme based on sandwich assay with HP1/HP2/DNA/AgNCs	Chen et al. (2015)
M-Pt NPs	Peroxidase	H_2O_2	0.05–20 U mL^{-1} (CA125) 0.008–24 U mL^{-1} (CA153) 0.02–20 U mL^{-1} (CEA)	0.002 U mL^{-1} (CA125) 0.001 U mL^{-1} (CA153) 7.0 pg/mL (CEA)	GE/GS/Ab1	CEA CA125 CA153 Sandwich immunoassay with M-PtNps/Ab2 label	Cui et al. (2014)
PtNPs	Peroxidase	H_2O_2	0.005–5.0 ng mL^{-1}	1.5 pg/mL	GCE/AuNPs/BSA-AFB_1	AFB_1 based on competitive immunoassay using anti-AFB_1-PtNPs/CoTPP/rGO as label	Shu et al. (2015b)
RuO_2/AuNP	Peroxidase/ Catalase	H_2O_2	0.1 nM to 30 mM	0.1 nM	GCE/Nafion/RuO_2NP/AuNP	H_2O_2	Anjalidevi et al. (2013)
HD-PtNDs@AuNRs	Peroxidase	H_2O_2	2.0–3800.0 μM	1.2 μM	GCE/HD-PtNDs@AuNRs	H_2O_2	Feng et al. (2014)
Au@Pt DNs/NG/ Cu^{2+}	Peroxidase	H_2O_2	0.5–50 ng mL^{-1}	0.167 pg/mL	GCE/Au@PDA/Ab1/BSA	Carcinoembryonic antigen (CEA) using Au@Pt DNs/NG/Cu^{2+}/Ab_2 as a label	Lv et al. (2018)
MoS_2–Au@Pt	Glucose oxidase	Glucose	10 μM-3 mM	1.08 μM	GCE/MoS_2–Au@Pt	Glucose	Su et al. (2018)
FeS or FeSe	Peroxidase	H_2O_2	5–140 μM (FeS) and 5–100 μM (FeSe)	4.3 mM (FeS) and 3 μM (FeSe)	FeS/GCE or FeSe/GCE	H_2O_2	Dutta et al. (2012)
$ZnFe_2O_4$/GQD	Peroxidase	H_2O_2	$10^{-16} - 10^{-9}$ M	6.2×10^{-17}M	GCE/GS/PdNws/S1/MCH	DNA using $ZnFe_2O_4$/GQDs/S3 as a label	Liu et al. (2014)
Co_3O_4NPs	Catalase	H_2O_2	10 μM-4 mM	4.4 μM	GCE/CO_3O_4NPs	H_2O_2	Mu et al. (2013)
CeO_2NPs	Catalase	H_2O_2	0.1pM-0.1 mM	–	GCE/CeO_2NPs	H_2O_2	Neal et al. (2017)
GQD	Peroxidase	H_2O_2	1–6.23×10^8 cfu mL^{-1}	5 CFU mL^{-1} (milk) 30 CFU mL^{-1} (serum)	Au/GQD/BSA/EA	*Y. enterocolitica bacteria*	Savas and Altintas (2019)
Co_3O_4NPs	Catalase	H_2O_2	5–250 μM	1.2 μM	ITO/PDDA/PbS/Co_3O_4	H_2O_2	Wang et al. (2019)
GBR	Catalase	H_2O_2	0.1–10 mM	0.063 mM	GCE/GBR/Nafion	H_2O_2	Singh et al. (2017)
Ag@Ag_2WO_4 NRs	Catalase	H_2O_2	62.34 μM- 2.4 mM	6.25 μM	Ag@Ag_2WO_4 NRs/GCE	H_2O_2	Koyappayil et al. (2020)
2D MnO_2 nanoflakes	Peroxidase Oxidase	Methylene blue	0.4–100 nM	0.25 nM	ITO	miRNA	Wu et al. (2021)
Pt@P-MOF(Fe)	Peroxidase	H_2O_2	$50 - 5 \times 10^5$HeLa cells mL^{-1}	20 cells	GCE/CGO/HpDNA/aDNA2	Telomers activity based on label approach	Ling et al. (2020)

(*continued on next page*)

Table 1 (*continued*)

Nanozyme	Pseudo-enzymatic activity	Substrate	Linear range	LOD	Sensor configuration	Target	Reference
Co-MOF	Glucose oxidase	Glucose	0.8 mM–16 mM	0.15 mM	CC/Co-MOF	Glucose	Wei et al. (2021a)
AuNFs/ Fe_3O_4@ZIF-8-MoS_2	Peroxidase	H_2O_2	5 μM–120 mM	0.9 μM	GCE/Fe_3O_4@ZIF-8-MoS_2/AuNFs	H_2O_2	Lu et al. (2020)
rGO/MoS_2/Fe_3O_4NP	Peroxidase	TMB	15-45 cells mL^{-1}	6 cells mL^{-1}	MGCE/rGO/MoS_2	Circulating tumor cells (CTCs) based on sandwich assay	Tian et al. (2018b)
Fe_3S_4–Pd	Peroxidase	H_2O_2	500 fg mL^{-1}-50 ng mL^{-1}	130 fg/mL	MGCE/Fe_3S_4–Pd/Ab1/BSA	Procalcitonin based sandwich immunoassay	Qu et al. (2020)
GNR@Pd SSs	Peroxidase	Hydroquinone	10–200 ng mL^{-1}	0.15 ng mL^{-1}	Au/DNA tetrahedron/BSA	Human epidermal growth factor receptor 2 based sandwich assay	Chen et al. (2019)
Fe_3O_4 MMIPs	Peroxidase	Thionine	2.85–160 μM (AChl), 0.53–20000 ng mL^{-1} (AChE), 22.76–400 ng mL^{-1} (ChOx), 4.08 nM–9.0 μM (H_2O_2)	0.86 μM (AChl), 0.16 ng mL^{-1} (AChE), 6.83 ng mL^{-1} (ChOx), 1.58 nM (H_2O_2)	GCE/Fe_3O_4 MMIPs	Acetylcholine (AChI), Acetylcholinesterase (AChE), Choline oxidase (ChOx), H_2O_2	Wang et al. (2017)
FeP-pSC_4-AuNPs	Peroxidase	H_2O_2	0.3–1.8 mM	25 μM	GCE/FeP-pSC_4-AuNPs	H_2O_2	Hu et al. (2021)
Au@PtNP/GO microbeads	Peroxidase	TMB	7 μM −1 mM	5.6 μM	ITO/Au@PtNP/GO microbeads	H_2O_2	Ko et al. (2019)
CuO NPs	Peroxidase	H_2O_2	50–7 × 10^3 cells mL^{-1}	27 cells mL^{-1}	GCE/rGO/AuNPs/MUC-1 aptamer	MCF-7 circulating tumor cells based on sandwich assay	Tian et al. (2018c)
Co_3O_4 NPs	Peroxidase	H_2O_2	5 × 10^{-13}–4 × 10^{-10} M	1.18 × 10^{-13} M	Au/COF-AI-ECL/Co_3O_4/MIP	Chloramphenicol	Li et al. (2021)
MOF@Pt@MOF	Peroxidase	H_2O_2	1 fM −1 nM	0.29 fM	GE/captureprobe@protectorB/MCH	Exosomal miRNAs based on label assay	Li et al. (2020)
Ag/ZnMOF	Peroxidase	DAB	0.5 nM–500 nM	0.18 nM	TM/WS_2 NA/Au–P1/BSA	Bleomycin	Kong et al. (2020)
MWCNT-avidin/RuNPs	Peroxidase	H_2O_2 Glucose	5.0 × 10^{-7}–1.75 × 10^{-3} M (H_2O_2) 2.0 × 10^{-5} –1.23 × 10^{-3} M (glucose)	65 nM (H_2O_2) 3.3 μM (glucose)	GCE/MWCNT-avidin/RuNPs GCE/MWCNTs-Av/RuNPs/biot-GOx	H_2O_2 Glucose	Gallay et al. (2020)
Hemin-doped-HKUST-1	Peroxidase	Dopamine	0.03–10 μM	32.7 nM	GCE/RGO/Hemin-doped-HKUST-1	Dopamine	Kang et al. (2021)
AuPt/ZIF-8–rGO	Peroxidase	H_2O_2	100 nM-18 mM	19 nM	GCE/AuPt/ZIF-8–rGO	H_2O_2	Zhang et al. (2019c)
CeO_2	Peroxidase Catalase Oxidase	H_2O_2	100 nm-20 mM	20 nM	Au/CeO_2	H_2O_2	Alizadeh et al. (2020)
ZIF-67/$Cu_{0.76}Co_{2.24}O_4$ NSs	Laccase SOD Peroxidase Glutathione peroxidase	3,4-dihydroxyphenylacetic acid	0.5–20 μM	0.15 μM	GCE	3,4-dihydroxyphenylacetic acid	Liu et al. (2020)
MWCNT/Mn-MPSA	SOD	$O_2^{\bullet-}$	0–1.817 mM	0.127 μM	SPCE/MWCNT/$Mn_x(PO_4)_y$/Nafion	$O_2^{\bullet-}$	Cai et al. (2018)
ZIF-67/Pt–Co PC	SOD	$O_2^{\bullet-}$	16–168 μM 168–1608 μM	0.118 μM	SPGE/ZIF-67/Pt–Co PC/Nafion	$O_2^{\bullet-}$	Li et al. (2019c)
NGS/PB	SOD	$O_2^{\bullet-}$	24–1456 μM	1.2 μM	SPGE/NGS/PB/Nafion	$O_2^{\bullet-}$	Liu et al. (2015)
Mxene-Ti_3C_2/ATP/$Mn_3(PO_4)_2$	SOD	$O_2^{\bullet-}$	2.5 nM to 14 μM	0.5 nM	GCE/Mxene-Ti_3C_2/ATP/$Mn_3(PO_4)_2$/Nafion	$O_2^{\bullet-}$	Zheng et al. (2019)
GNP/Cu-Cys	SOD	$O_2^{\bullet-}$	3.1–326 μM	2.8 μM	CP/GNP/Cu-Cys	$O_2^{\bullet-}$	Dashtestani et al. (2015)
DNA-based $Mn_3(PO_4)_2$	SOD	$O_2^{\bullet-}$	1.67 − 1.44 × 10^3 *nM*	1.67 nM	$Mn_3(PO_4)_2$–DNA/CNF/GCE	$O_2^{\bullet-}$	Zou et al. (2019)
$MnTiO_3$	SOD	$O_2^{\bullet-}$		1.54 nM	GCE/$MnTiO_3$/Nafion	$O_2^{\bullet-}$	

(*continued on next page*)

Table 1 (*continued*)

Nanozyme	Pseudo-enzymatic activity	Substrate	Linear range	LOD	Sensor configuration	Target	Reference
			5.75–230 nM, 230–15467.5 nM, 15467.5–24955 nM				Zhao et al. (2019a)
Mn-MPSA-PCC	SOD	$O_2^{\bullet-}$	–	0.063 μM	SPE/Mn-MPSA-PCC	$O_2^{\bullet-}$	Cai et al. (2020)
$Mn_3(PO_4)_2$/MXene	SOD	$O_2^{\bullet-}$	5.75 nM to 25.93 μM	1.63 nM	GCE/$Mn_3(PO_4)_2$/MXene/Nafion	$O_2^{\bullet-}$	Zhao et al. (2021)
					PE/$Mn_3(PO_4)_2$/MXene		
N-HMCS	SOD	$O_2^{\bullet-}$	20–480 μM	2.2 μM	N-HMCS/SPCE/Nafion	$O_2^{\bullet-}$	Liu et al. (2017)

nanospheres which exhibited catalase-like, peroxidase-like, glutathione peroxidase-like and laccase-like activities. The amperometric responses for DOPAC were linear from 0.5 to 20 μM, with selective performance towards interfering species as UA, AA, dopamine (DA), epinephrine (E), norepinephrine (NE) and 5-hydroxytryptamine (5-HT) (Fig. 3A–b)). Considering the variety of MOFs, metal centers, and ligands, it is possible to design more efficient and stable nanozymes to be applied in POC testing. Wei et al. (2021a) developed a cobalt MOF (Co-MOF) modified carbon cloth/paper electrochemical analytical chip for nonenzymatic detection of glucose (Fig. 3B–c)). Co-MOF maintained a robust activity during 2 months at ambient surroundings which is a critical requirement for POC testing. Rapid on-chip detection of glucose demonstrated a high sensitivity and selectivity towards interfering species (KCl, AA, fructose (Fru), sucrose (Suc), lactose (Lac), urea, L-tryptophan(L-Trp)) in multiple complex bio-matrixes (serum, urine and saliva) (Fig. 3B–d)).

In the perspective of promising electrochemical platforms, multi-enzyme activity nanozymes may be pointed out as a trendy system (Alizadeh et al., 2020; Anjalidevi et al., 2013; Liu et al., 2020; Wu et al., 2021). They may provide the possibility of multiplexed detection exploring each type of specific mimic activity perform by multi-enzyme activity nanomaterials. For instance, the dual enzyme property of 2D MnO_2 nanosheets demonstrated a high activity to catalyze the oxidation of O_2 into reactive oxygen species (ROS). Therefore, Wu et al. (2021) investigated their oxidase-like activity towards oxidation of TMB, OPD, ABTS (3-ethylbenzthiazoline-6-sulfonic acid) in the presence of O_2 (Fig. 3C–e). Then, the yielded H_2O_2 was applied for the subsequent peroxidase-like catalytic oxidation (Fig. 3C–e). This nanozyme was used to detect microRNA based on its unique response to single stranded DNA (ssDNA) over doubled stranded DNA (dsDNA). Additionally, the formed ROS could eliminate the electroactive methylene blue (MB) in solution through catalytic oxidation. The interaction with DNA and the catalytic oxidation of MB by 2D MnO_2 nanosheets were the key for this selective approach towards several different microRNAs with a low limit of detection of 0.25 nM (Fig. 3C–f).

3.1.1. Labeling detection in nanozyme-based electrochemical biosensors

Label-based approaches incorporate an extrinsic molecule which is chemically or transiently attached to the analyte to detect its presence or activity, and which may change its inherent properties (Syahir et al., 2015). In the electrochemical biosensors' scenario, nanozymes may act as probe-labels with catalytic performance, usually applied to detect non-electroactive species (Fig. 4). In terms of convenience, it seems less complicated to design label-free sensors, since more preparation steps are necessary leading to a time-consuming procedure in addition to inherent higher costs associated with complex labels, and lack of scalability. However, those disadvantages may be compensated considering an increased sensitivity, lack of cross-reactivity, or interference effects by label-based sensing approaches (Koyappayil and Lee 2021). Labeled sensors may be preferred over label-free configurations when preparation facilities and trained personnel are available. Electrochemically active probe labeling is particularly appealing due to its high sensitivity and robustness in addition to the possibility of the system miniaturization. However, the labeling process may lead to a background produced by label molecules since they have potential to introduce artifacts by inactivating the analyte or diminishing its capacity to interact (El-Gewely 2003). The combination of electrochemical transducing systems and electroactive-based labels, such as nanozymes, have achieved selective and sensitive determination of several biomolecules (Bhattacharjee et al., 2018; Chen et al. 2015, 2019; Cui et al., 2014; Li et al. 2019a, 2020; Ling et al., 2020; Liu et al., 2014; Lv et al., 2018; Qu et al., 2020; Shu et al., 2015b; Tian et al. 2018b, 2018c).

Among labeling methods, sandwich assays are the most frequently adopted in electrochemical biosensors. In a sandwich assay the analyte is bound to a recognition molecule 1, then a recognition molecule 2

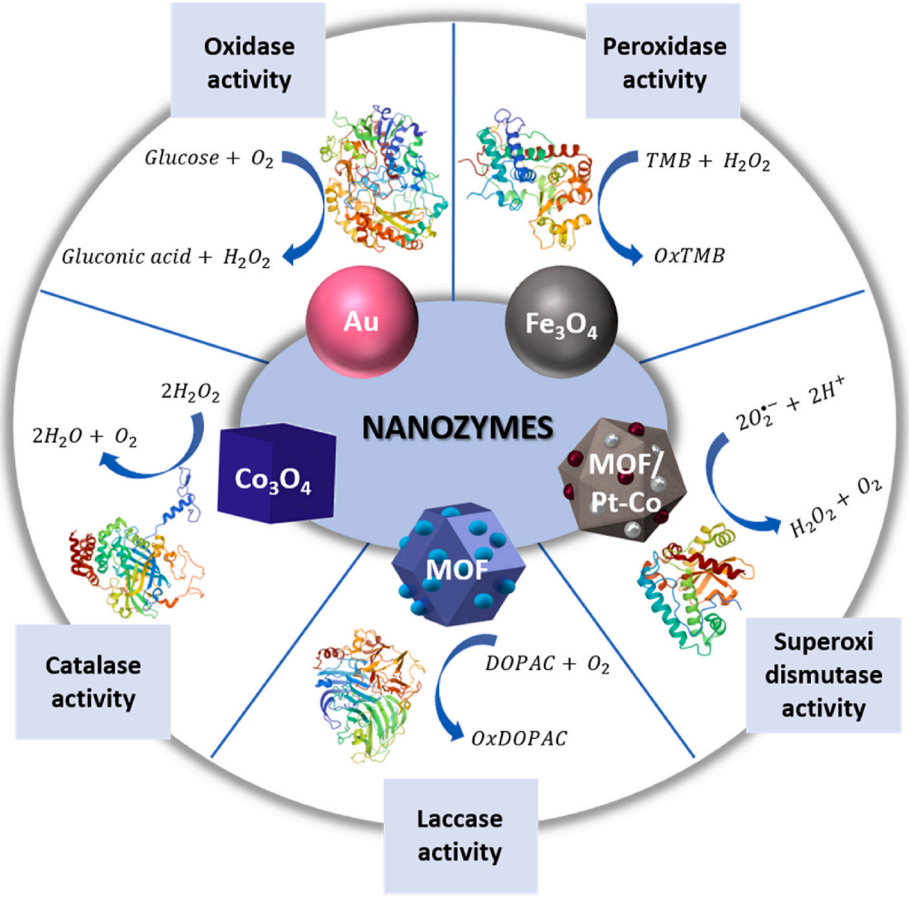

Fig. 2. Scheme of reactions catalyzed by different nanozymes.

labeled with a detectable signal is bound to the analyte (Xia et al., 2018). This strategy is highly applied to design antibody-based immunoassays. A sandwich-type electrochemical immunosensor was proposed based on a special signal-off mode for the sensitive detection of procalcitonin (PCT) biomarker by using Fe_3S_4–Pd NPs as a signal indicator and matrix and functionalized pineal mesoporous bioactive glass (PBG) as the label for signal amplification (Fig. 4A–a) (Qu et al., 2020). The authors achieved a linear detection range from 500 fg/mL to 50 ng mL^{-1} of PCT and a low limit of detection of 130 fg/mL, which promoted a promising detection method for sensitive detection of other biomarkers (Fig. 4A–b). Furthermore, Lv et al. (2018) developed a sandwich-type electrochemical immunosensor for early detection of carcinoembryogenic antigen (CEA), a tumor marker. They used cubic Au@Pt dendritic nanomaterial functionalized with nitrogen-doped graphene loaded with copper ions (Au@Pt DNs/NG/Cu^{2+}) with peroxidase-like activity conjugated with a secondary anti-CEA as a label (Fig. 4D–g). The Au@Pt DNs/NG could effectively electrocatalyze H_2O_2 reduction along with signal amplification promoted by Cu^{2+} ions. As shown in Fig. 4D–g (curve a), there is no obvious current response of the immunosensor without Antibody 2 (Ab2) labeled probe, indicating that the background current response cannot affect the precision of the immunosensor. The Au@Pt DNs/NG/Cu^{2+}-Ab2 label displayed the highest current change in comparison with other sensor configurations, obtaining a limit of detection of 0.167 pg/mL.

In the case of electrochemical detection of DNA strands, it is possible to rely on the intrinsic redox-active properties of DNA/RNA bases, especially by using the guanine electrochemical oxidation signal (Palecek and Bartosik 2012; Palecek et al., 2014). However, to achieve high sensitivity it may be necessary to amplify the signal using labels. Li et al. (2020) reported an electrochemical strategy based on the cascade primer exchange reaction (PER) with MOF@Pt@MOF nanozyme for ultrasensitive detection of exosomal miRNA. Under the catalysis of the nanozyme, hydrogen peroxide was decomposed, thus producing an amplified electrochemical signal (Fig. 4B–c). The correlation between the current signal change and the logarithm of miRNA-21 concentration displayed a good linear relationship in the range from 1 fM to 1 nM (Fig. 4B–d) with a low limit of detection of 0.29 fM. High selectivity was demonstrated in the presence of interfering species at 1 nM, together with the target at 10 pM (Fig. 4B–d). Moreover, a simple and sensitive strategy for the detection of telomeres activity was proposed by (Ling et al., 2020) based on Pt NPs decorated on MOF surface as a signal probe. Exonuclease III (Exo III) acted as recycling amplification and structure switch of triple-helix DNA as signal transduction (Fig. 4C–e). In Fig. 4C–f), it can be seen that the current response increased with the increasing of cells concentration, due to more hairpinDNA (HpDNA) being released, leading to more HpDNA-cDNA being formed and allowing more Pt@P-MOF(Fe) to bind on electrode surface. The peak current was well correlated to the logarithm of cell concentration from 50 to 5×10^5 cells/mL, with a limit of detection of 20 cells. These results indicated a synergy between MOF structure and Pt NPs, improving the electrochemical signal and its sensitivity.

Despite the advantages offered by label-based electrochemical sensor, numerous obstacles remain for the commercial utilization of these ultrasensitive sensors, such as the lack of reproducibility and scalable production. More systematic studies concerning the system optimization and robustness are still required (Koyappayil and Lee 2021).

Although the catalytic performance of nanozymes is exceptional, they have limited selectivity, which may be the key point to use nanozymes in commercial sensing devices (Gooding 2019). Engineering their

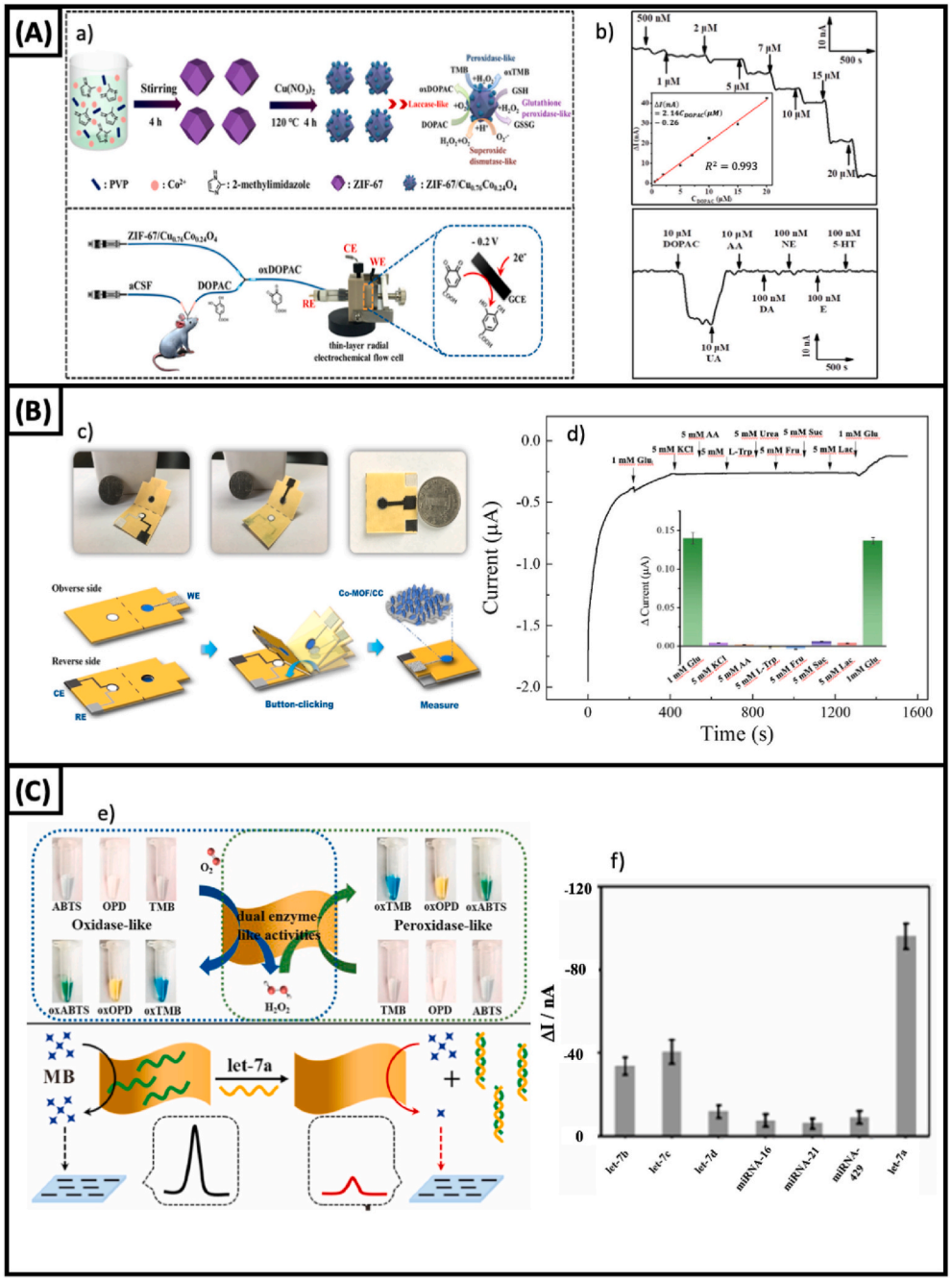

Fig. 3. A). a) Scheme of ZIF-67/$Cu_{0.76}Co_{2.24}O_4$ nanospheres fabrication and electrochemical detection platform for DOPAC. b) Amperometric responses for different concentrations of DOPAC (top); and amperometric response recorded DOPAC in presence of different species (bottom). Adapted with permission from reference Liu et al. (2020). Copyright (2020) American Chemical Society. **B).** c) Photographs of Co-MOF based sensor and the assay procedure. d) Amperometric response of Co-MOF cloth to different interfering species. Adapted from reference (Wei et al., 2021b), Copyright 2020, with permission from Elsevier. **C).** e) Schematic interaction of 2D MnO_2 nanoflakes and enzymatic substrates based on oxidase-like and peroxidase-like activities (top), and the sensing principle of ssDNA/MnO_2-based biosensor for miRNA assay (bottom). f) Selectivity assay of ssDNA/MnO_2-based electrochemical biosensor. Adapted from reference (Wu et al., 2021), Copyright 2020, with permission from Elsevier.

activity and selectivity should be prioritized though surface coating and modification, composition regulation, formation of complexes and hybrids, etc (Wu et al., 2019b). Owing to the limited specificity of inorganic materials, several nanozymes turned out to exhibit multienzyme activities which may hamper the sensitive substrate-specific reaction of the target molecule (Wang et al., 2020d). Only a few studies have been made focusing on the improvement of selectivity of nanozymes. Strategies to increase their selectivity concern the design of substrate-binding pockets, the imitation of the cofactor structures, and surface modification (Fan et al., 2016; Huang et al., 2017; Kim et al., 2019b; Zhang et al., 2017). For instance, the iron oxide nanozyme is a classical nanomaterial with intrinsic peroxidase-like activity, but it was also found to have catalase-like activity in neutral/basic pHs (Chen et al., 2012). In an attempt to increase the selectivity of Fe_3O_4 NPs, their surface was modified with a single amino acid (histidine) to mimic the architecture of the active site of natural peroxidase (Fan et al., 2016). The introduction of histidine improved the peroxidase-like activity by increasing the affinity for H_2O_2 via hydrogen bond formation between the imidazole group of histidine and H_2O_2.

Recently, single-atom catalysts have emerged as a rising star class among catalysts materials, based on the anchoring of isolated metal atoms with catalytic activity onto a solid support (Zhang et al., 2020c). This class of catalysts possesses homogeneously dispersed catalytic sites, which offer possibilities for precise control of geometric and electronic properties of catalytic active sites. Thereby, these homogeneously dispersed active sites provide high selectivity and catalytic activity. The single-atom catalyst approach has enabled the development of a peroxidase-like nanozyme with both improved activity and selectivity. Inspired by the shape of the heme cofactor present in the active site of natural peroxidase, Lee's group rationally designed a heme

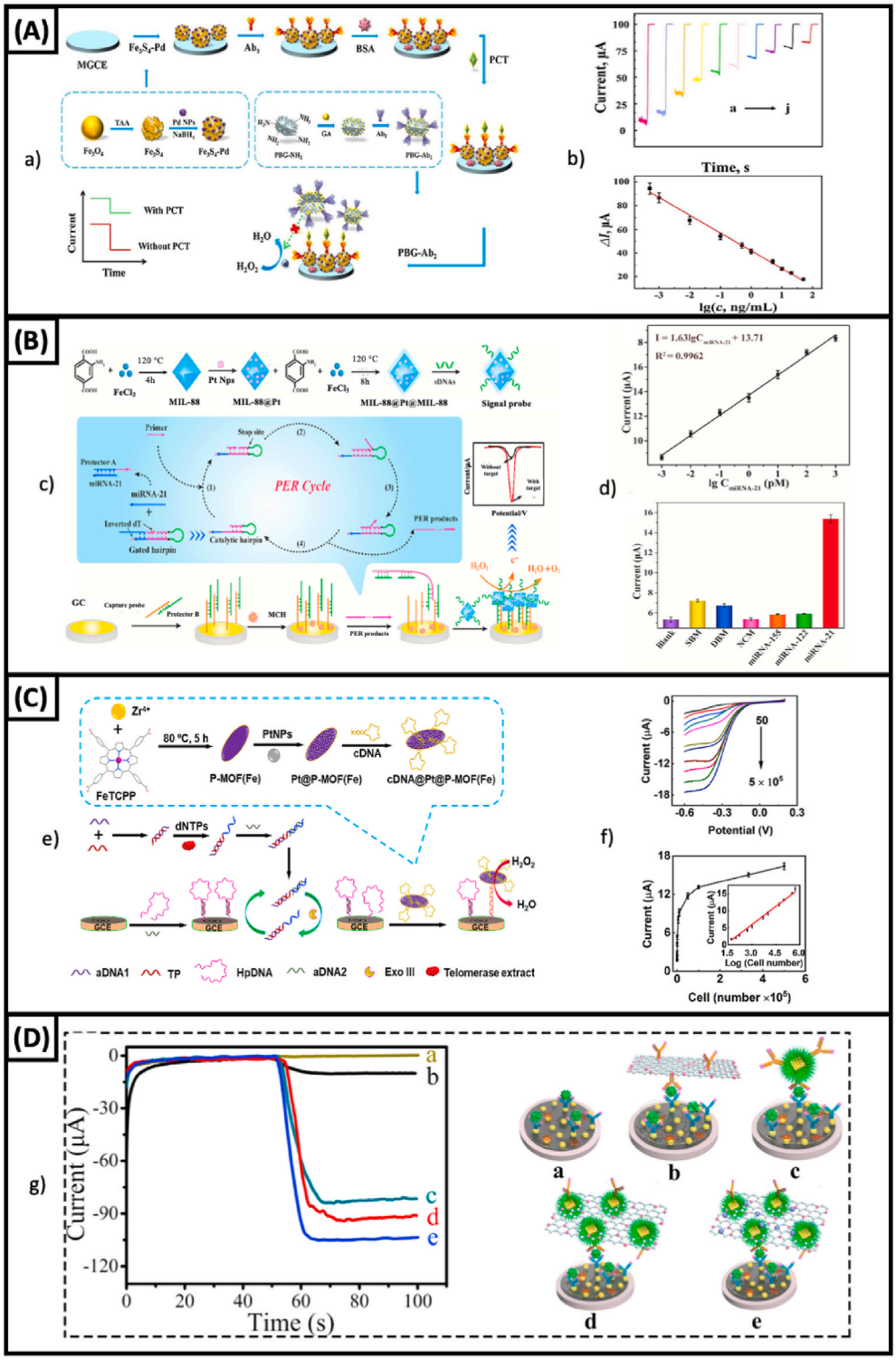

Fig. 4. A). a) Schematic presentation of EC immunosensor fabrication for procalcitonin detection (PCT). b) Amperometric i-t curves and the calibration curve for PCT detection. Adapted from reference (Qu et al., 2020), Copyright 2020, with permission from Elsevier. **B).** c) Principle of the electrochemical biosensor based on the cascade primer exchange reaction (PER) for the detection of exosomal miRNA-21. d) Linear relationship of DPV signals vs. lgCmiRNA-21 (top); interference studies at different miRNAs (bottom). Adapted from reference (Li et al., 2020), Copyright 2020, with permission from Elsevier. **C).** e) Working sensing principle for the detection of telomerase activity. f) Linear sweep voltammograms for a range of HeLa cell number; and the dependence of LSV peak currents on HeLa cell concentration. Adapted from reference (Ling et al., 2020), Copyright 2019, with permission from Elsevier. **D).** g) Working principle of label-based immunosensor and current responses for the detection of CEA without label (a), and different signal labels (b–e). Adapted from reference (Lv et al., 2018), Copyright 2018, with permission from Elsevier.

cofactor-resembling Fe–N_4 single site-embedded graphene (Kim et al., 2019b). This nanozyme exhibited 5 million times higher activity per iron ion when compared to Fe_3O_4 NPs and showed exceptional specificity toward H_2O_2. Notably, when Fe or N were doped alone or when Fe was replaced with another transition metal in the Fe–N_4 site, the activity was negligibly enhanced. The authors previously reported a N- and B-codoped graphene with peroxidase-like activity without oxidase activity, however its activity was not sufficient for use in versatile applications (Kim et al., 2019a) and K_{cat}/K_m was lower than the one for Fe–N_4-rGO.

According to Gooding (2019), it could be hard to imagine that nanoparticles with limited control over the molecular architecture of the active site, and even less over the solution environment could compete with natural enzymes for selectivity. On the other hand, the counter-argument to use nanozymes is their superior stability over natural enzymes. The future of nanozymes aims for increased selectivity towards advances in synthesis to surpass enzymes in sensing applications. In this scenario, MIPs and synzymes offer more complex

Table 2
Biomimetic electrochemical sensors employing Synzymes, MIPs, and Metal complexes.

Biomimetic class	Material	Pseudo-enzymatic activity	Target analyte	Sensor configuration	Linear range	LOD	Remarks	Reference
Synzymes	PEI-NH_2	Oxalacetate decarboxylase	Oxalacetate	Sandwiched PEI-NH_2 in gas sensing membrane	0.79–5.6 mM	–	Oxalacetate as substrate	Ho and Rechnitz (1987)
	PVI	Fructosylamine dehydrogenase	Fructosyl valine	Carbon paste and PVI	20 μM- 0.7 mM	20 μM	Fructosyl valine as substrate	Sode et al. (2001)
	PMP complex Cu	Phosphatases	PO_4^{3-}	Pt/PMP complex Cu	1 nM-20 mM (ATP) 5 μM −20mM (pyrophosphate)	–	ATP Pyrophosphate as substrate	Ikeno and Haruyama (2005)
	PMP complex Cu	Phosphatases	PO_4^{3-}	PMP complex Cu membrane-coated GCE	–	–	Phosphoric substances as substrate	Ikeno et al. (2007)
	PMP complex Cu	Phosphatases	PO_4^{3-}	Polyacrylamide/PMP complex Cu membrane-coated GCE	–	–	AMP; ADP; ATP; pyrophosphate as substrate	Ikeno et al. (2009)
	PHA	Acetylcholinesterase	Paraoxon-ethyl, fenitrothion and chlorpyrifos	SPE/PHA/mPEG	1.0–10.0 μM	0.36 μM (paraoxo-ethyl); 0.61 μM (fenitrothion); 0.83 μM (chlorpyrifos)	Acetylthiocholine as substrate	Sgobbi and Machado (2018)
	PPy-IMZ	Alkaline phosphatase	Diethyl 2,4-dinitrophenylphosphate	PPy-IMZ/Nafion/ITO	–	–	Diethyl 2,4-Dinitrophenylphosphate as substrate	Hryniewicz et al. (2020)
MIPs	Dopamine	–	Human hemoglobin	FTO/CdS/TiO_2/MIP	0.01–100 ng mL^{-1}	0.53 pg/mL	MIP-CdS/TiO_2 nanocomposites integration	Gao et al. (2021)
	$CuFe_2O_4$-based polymer	–	IgG	GCE/MoS_2@N-GQDs-IL/MMIP	0.1–50 ng mL^{-1}	0.02 ng mL^{-1}	Integration of multiple materials for signal amplification	Axin Liang et al. (2021)
	Methacrylic acid	–	BRCA-1	GCE/RGO/Au/MIP	10 fM-100 nM	2.53 fM	Rhodamine as MIP template	You et al. (2018)
	o-PD and scopoletin	–	Glucose	GW/Au-MIP	1.25 nM-2.56 μM	1.25 nM	Non-enzymatic MIP-Nanozyme integrated glucose sensor	Sehit et al. (2020)
	o-PD	–	Ni^{2+}	GCE/MIP	3 pM-6 nM	1.01 pM	Ni-DMG as MIP template	Yang et al. (2016b)
	UPDHS	–	Proteins	GE/BSA@UPDHS-NPs	0.01 fg mL^{-1}-10 pg/mL	–	BSA as MIP template	Zhao et al. (2019b)
	Methacrylic acid	Peroxidase	Acetaminophen	GCE/MWCNT-MIP	10–90 μM	1.1 μM	Peroxidase-like catalysis	Moretti et al. (2016)
Metal complexes	Mn(III) *meso*-tetra(*N*-methyl-4-pyridyl) porphyrin	Non-heme manganese catalases	Serum H_2O_2 and glucose	GCE/Metal complex/Nafion	40 μM-1 mM (H_2O_2) 0.1–2 mM (glucose)	0.5 μM (H_2O_2) 8 μM (glucose)	Application in the presence of oxygen	Peng et al. (2020)
	β-cyclodextrin complex	Esterase/Cytochrome P450	R and S-Clopidogrel	Modified carbon paste electrode	2 μM-0.2 mM	4.87×10^{-7} M	Enantioselectivity	Upadhyay et al. (2019)
	$[Mn^{III/IV}(\mu\text{-}O)(phen)_2]_2(ClO_4)_3$	Oxidase	Acetazolamide	Modified carbon paste electrode	5–25 nM	4.76 nM	Multinucleated Mn complex	Machini and Teixeira (2016)
	Cu(II)-poly-L-histidine	–	Salvianic acid A	PtE/Complex	0.4–1000 μM	0.037 μM	Synergetic effect between MWCNT and Cu-complex	Wang et al. (2018b)
	Fe(II)-BTC	–	NO photorelease	GCE/Fe(II)-BTC film	18 nM-9 μM	7.2 nM	High stability in the pH range of 5.0–8.0	Huang et al. (2020)
	Ni(II)-TBLPyP	Cytochrome P450	Dopamine	GCE/Ni(II)-TBLPyP film/rGO	0.01–200 μM	1.40 nM	Synergetic effect between rGO and Ni-complex	Yan et al. (2016)
	Cu(II)-4,4-dimethyl-3-thiosemicarbazide	–	MicroRNA-21	MGCE/MCH/Fe3O4/HCP/microRNAs/HDNA1/HDNA2/Cu(II) complex	100 aM-100 nM	33 aM	Cu-complex as both enzyme mimic and intercalator in a magnetic sensor	Tian et al. (2018a)

tridimensional structures leading to enhanced selectivity and specificity due to the catalytic functional groups and internal microenvironments to attract the substrate. Considering the electrochemical sensing platforms, other issues behind the use of nanozymes are associated with poor reproducibility in their synthesis to guarantee controlled size, shape and porosity from different batches (Mahmudunnabi et al., 2020). Standardization of effective protocols are required. In addition, biofouling of the electrode surface also hampers the potentiality to spread the nanozyme-based electrochemical biosensors to perform analysis in bodily fluids or other complex matrices. Several compounds present in these matrices may adsorb on the electrode surface via nonspecific interactions affecting the electrochemical signal. Strategies to address this issue remain highly challenging within the electrochemical sensing community.

4. Synzymes – polymers with enzyme-like activity

Another turning point in Biomimetic Chemistry emerged with the development of synzymes which are polymers with enzyme-like activities first reported by Klotz et al. (1971). Their endeavors to achieve synthetic polymers with catalytic behavior were strongly guided by previous studies regarding the binding of small molecules by proteins (Lefever and Goldbeter 1978). Accordingly, the authors obtained a synthetic polymer containing dodecyl groups (which are able to bind small substrate molecules) in addition to methyleneimidazole side chains (as nucleophilic catalytic sites) linked to a polyethyleneimine (PEI) framework. This macromolecule was able to catalyze the hydrolysis of uncharged nitrophenyl esters in water at pH 7 with rates considerably higher in comparison with other synthetic substances under similar conditions (Klotz et al., 1971). Exploratory mechanistic studies revealed that the hydrolysis proceeds along a pathway similar to that of hydrolytic enzymes, such as α-chymotrypsin.

Taking into account that all enzymes are macromolecules, one may assume that a polymer framework could also provide an auspicious foundation for a synthetic catalytic entity. Generally, the precursor for a synzyme may itself be a protein or any synthetic polymer. Synzymes are designed in such a manner that they have at least two structural regions, one for the binding of the substrate and the other for the actual catalytic function (Suh 2001). The catalytic performance of synzymes can be particularly inefficient depending on the surrounding conditions. However, it can be enhanced by modification of the local microenvironment.

In order to obtain synzymes, several types of non-natural polymers are readily available by simple polymerization processes, and many more could be developed via subsequent functionalization. They include both linear and branched systems, considering the number of catalytic groups and their distribution as the key elements. Prominent among the synthetic polymers is polyethylenimine (PEI), available as a highly branched structure containing a mixture of primary, secondary, and tertiary amine centers, which are protonated to various extents under physiological conditions (Breslow 2005). At pH 7 the amine and ammonium moieties of the structure offer an array of potential nucleophiles, general bases and acids, inserted into a polycationic backbone capable of binding anionic substrates and transition states (Kirby and Hollfelder 2009). PEI-based synzymes create supramolecular systems bearing a specific local environment, which resemble the active site of

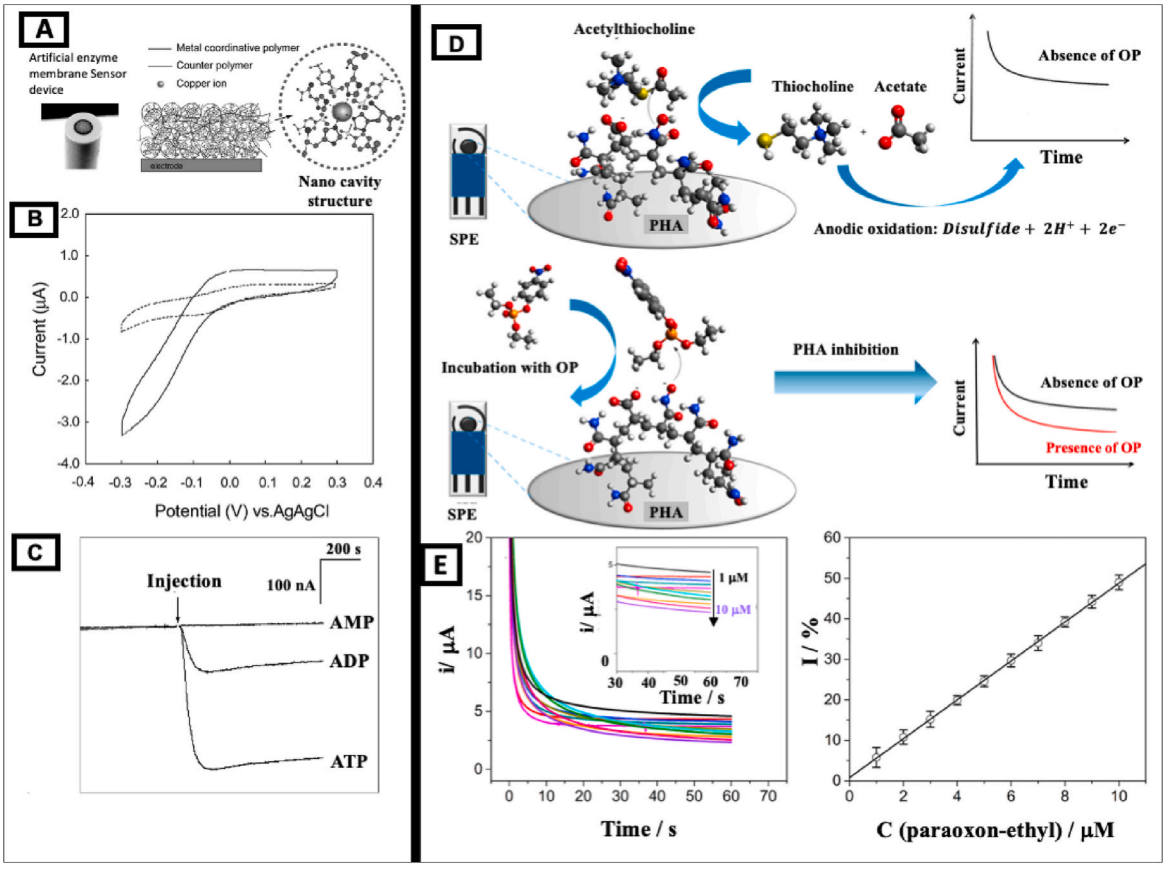

Fig. 5. **A)** Scheme of the artificial enzyme membrane sensor. **B)** Cyclic voltammograms of the artificial enzyme sensor in the presence (solid line) and in the absence of ATP. **C)** Sensor response curves for different adenosine phosphates recorded at constant potential. Adapted with permission from (Ikeno et al., 2007). Copyright (2007) American Chemical Society. **D)** Scheme of sensing principle for the biomimetic electrochemical sensor based on the modified polyacrylamide. **E)** Chronoamperograms obtained at SPE/PHA/mPEG sensor at different concentrations of paraoxon-ethyl in the presence of ATCh; and the analytical curve. Reprinted from reference (Sgobbi and Machado 2018), Copyright 2017, with permission from Elsevier.

enzymes in the presence or absence of natural or artificial cofactors (Avenier et al., 2007; Avenier and Hollfelder 2009; Chevalier et al., 2018; Roux et al., 2015). Hollfelder's group reported that a modified PEI containing guanidinium, dodecyl and benzyl groups was able to catalyze the transesterification of 2-hydroxypropyl-4-nitrophenyl phosphate (HPNP) in the absence of metal ions with a rate acceleration k_{cat}/k_{uncat} of 4.6×10^4 (Avenier et al., 2007). Guanidinium groups are familiar features of phosphatase active sites, such as ribonuclease A and alkaline phosphatases, and are well-known as phosphate binding anchors, which increase the affinity of negatively charged phosphate substrates. Besides, the addition of dodecyl and benzyl groups as the hydrophobic components brings a suitable reaction medium emulating the interior of a protein. Later, Hollfelder's group also demonstrated that the combination of metal ion cofactors and the adjustment of synzyme microenvironments could provide catalysis due to hydrophobic and metal cofactors synergetic effects (Avenier and Hollfelder 2009). A metal-coordinated synzyme based on PEI functionalized with alkyl and guanidinium moieties exhibited accelerated phosphate transfer by 10^8. The identity of the metal ions influenced the magnitude of rate enhancement, among zinc showed superior performance. Generally, zinc redox inertness, lower toxicity and its low metal-hidroxo pKa compared to other metals have been discussed as the reasons why many phosphatases contain Zn^{2+} (Weston 2005). Alternatively, Roux et al. (2015) described an artificial reductase based on modified PEI also derivatized with guanidinium and octyl groups to bind the phosphate group of the flavin mononucleotide. This macromolecule was capable of

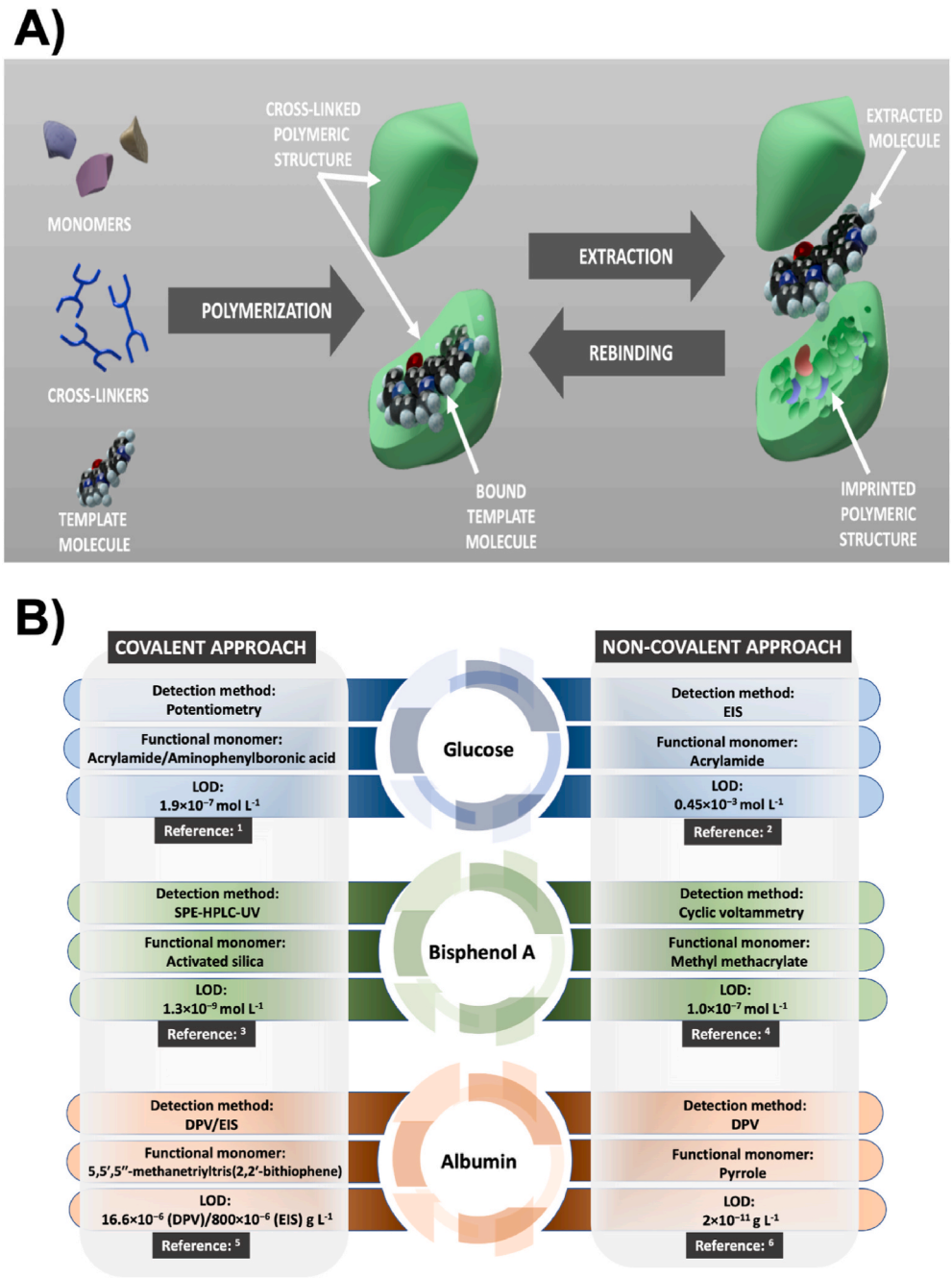

Fig. 6. A) Simplified steps of a traditional synthesis of a molecularly imprinted polymer. **B)** Comparison between the covalent and non-covalent approaches employed in MIP based electrochemical biosensors/analytical methods. References: [1] (Kim et al., 2017) [2] (Wu et al., 2019a) [3] (Hu et al., 2016) [4] (Zhu et al., 2014) [5] (Cieplak et al., 2015) [6] (Xia et al., 2016).

oxidizing NADH and promptly delivering single electrons towards redox cofactors, such as Mn(III) porphyrin, similar to the activity of cytochrome P450 reductase. Remarkably, this synzyme highly resembles the activity of natural reductases with kinetic parameters three orders of magnitude lower than the natural counterparts. Recently, Chevalier et al. (2018) demonstrated that under aerobic conditions, similar artificial flavoenzymes made of flavin cofactor incorporated into PEI catalyze the oxidation of NADH and perform aerobic Bayer-Villiger reactions in water with high selectivity. These artificial enzymes paved the way to the development of new environmentally friendly catalysts capable of using dioxygen in water.

The functional groups inserted in the PEI backbone chain are the key parameters to ascribe specifical catalytic behavior to the designed synzyme, allowing them to mimic different types of enzymes. For instance, PEI modified with orientated salicylate groups led to the hydrolysis of γ-globulin similarly to proteases (Suh and Hah 1998). On the other hand, PEI functionalized with imidazole groups promoted dephosphorylation reactions which is a particular class of vital biological reactions related with phosphorylated structures such as DNA and RNA (Ferreira et al., 2015b). The cooperative effects related to substrate activation performed by amine groups and further nucleophilic reaction towards imidazolium rings enabled the catalysis. More recently, a water-soluble imidazolium-functionalized PEI was applied as a metal-free catalyst to promote the multicomponent synthesis of isoxazole-5(4H)-one (ISX) derivatives (Oliveira et al., 2021). The precursors 1,3-carbonyl (electrophile), hydroxylamine (nucleophile), and ethyl acetoacetate were mixed with imidazolium-modified PEI obtaining a ISX derivative towards a catalytic multicomponent reaction. The interaction with this synzyme facilitates the condensation reaction between the hydroxylamine and the activated 1,3-carbonyl which further undergoes cyclization yielding ISX by ethanol elimination. Most previously available methodologies to obtain ISX derivatives do not allowed the reuse of the catalytic system or required metals (usually toxic ones) to perform multicomponent reactions. Aside from PEI-based synzyme, natural polymers also can be used as frameworks to configurate artificial enzymes, such as gum Arabic which is a natural biocompatible polymer obtained from *Acacia* tree exudates. Ferreira et al. (2015a) proposed the rational anchoring of highly reactive imidazole groups on gum Arabic as an artificial nuclease to promote nucleophilic catalytic dephosphorylation of organophosphates and DNA.

Another strategy to design efficient synzymes is related to the incorporation of polyoxometalates (POMs), a large group of anionic polynuclear metal–oxo clusters with discrete and chemically modifiable structures, which may allow oxidation catalysis (Gumerova and Rompel 2020). Haimov et al. (2004) combined alkylated PEI and polyoxometalates yielding water-soluble synzymes with hydrophobic regions that enabled the aqueous biphasic selective oxidation of very hydrophobic substrates with hydrogen peroxide. Meanwhile, in the presence of unmodified PEI the conversions were negligible, particularly in the case of the alkene bond cleavage oxidation. A further milestone in synzyme-based systems was reported by Gobbo et al. (2020) regarding a new type of catalytic microcompartment with multi-functional activity which provided a step towards the development of protocell reaction networks (Gobbo et al., 2020). Thereby, a membrane-free molecularly crowded PDDA/ATP (polydiallydimethylammonium chloride and adenosine 5′-triphosphate) coacervate microdroplets were spontaneously reconfigured into a catalytic membrane-bounded coacervate vesicles in the presence of a bioinspired Ru(IV)-based polyoxometalate ($Na_{10}[Ru_4(\mu\text{–}O)_4(\mu\text{–}OH)_2(H_2O)_4(\gamma\text{–}SiW_{10}O_{36})_2]$; Ru_4POM) and sodium phosphotungstate ($[PW_{11}O_{39}]^{7-}$; PTA) polyanionic clusters. The catalase-like activity was determined by incubating the synzyme active protocells (Ru_4PCVs) with H_2O_2, followed by measurements of the O_2 produced. Then, kinetics studies showed a second order rate constant of $43.0 \times 10^{-3}\ M^{-1}s^{-1}$. In contrast, no catalytic activity was observed when ruthenium-free PTA coacervate vesicles were exposed to H_2O_2 under identical conditions.

Synzymes exhibit alluring attributes to be used in electrochemical biosensors in the replacement of natural enzymes (Table 2). They are capable of significantly accelerate numerous types of reactions as well as bringing selectivity, crucial features for the development of an electrochemical sensing platform. Moreover, it is possible to take advantage of the chemical groups inserted along the polymeric framework to immobilize the synzyme onto electrode surfaces. The first synzyme-based sensor was proposed by Ho and Rechnitz (1987) for the potentiometric detection of oxaloacetate. They used an artificial enzyme based on partially quaternized PEI in which 10% of the residues are retained as primary amines. This modified PEI catalyzed the decarboxylation of oxaloacetate; and the rates of decarboxylation fit equations for saturation kinetics similar for those for natural oxalacetate decarboxylase enzyme (Spetnagel and Klotz 1976). Thereby, a synzyme-based electrode was fabricated by sandwiching the artificial enzyme between dialysis membranes held at the tip of a pCO_2 membrane electrode. Remarkably, the artificial enzyme electrode yielded a near Nernstian response slope for a certain range of oxaloacetate concentrations throughout the 6-month test period. On the other hand, the operating lifetime of the natural enzyme-based sensor was lower than one week. Moreover, the synzyme-based sensor was quite selective since it exhibited only a mild response for the β-ketoglutaric acid among the 13 interferents evaluated. These findings bespeak that is possible for synzymes to be synthesized to meet specific biosensor needs.

Sode et al. (2001) developed a biomimetic catalyst based on fructosylamine dehydrogenase to oxide fructosyl valine (Fru-val) substrate. They were inspired by the presence of histidine (His) residues in the catalytic center of oxidoreductases which play the role of the general base. Therefore, they chose polyvinylimidazole (PVI) which contains imidazole moieties to mimic His residues as a model catalytic center for the construction of an artificial fructosylamine dehydrogenase. The catalytic performance of PVI towards Fru-val oxidation was demonstrated by colorimetric assay in the presence of an electron acceptor (1-methoxyphenazinemethosulphate). Then, they constructed an amperometric sensor by mixing PVI with carbon paste for the measurement of Fru-val. The electrochemical measurement was based on the re-oxidation of the reduced 1-methoxyphenazinemethosulphate, which resulted from the oxidation of Fru-val. However, a potential instability of the system may be pointed out as the electron acceptor. On the other hand, PVI itself is stable and can operate at higher temperatures and in the presence of denaturants or proteases.

Haruyama's group designed a polymer-metal-functional polymer (PMP) complex to be applied in the detection of biologically relevant phosphoric substances (Ikeno et al. 2007, 2009; Ikeno and Haruyama 2005). They synthesized PMP using polyhistidine (coordinative polymer), polystyrene sulfonate (functional polymer) and Cu^{2+} (Ikeno and Haruyama 2005). Simultaneously, multiple Cu^{2+}-coordinated nanocavities are formed in the matrix, and the functional polymer binds to the coordinative polymer to constitute a polyion:polyion complex. Styrene residues provide hydrophobic and electrophilic conditions within the nanocavities which are significant for mimicking the structure of an artificial enzyme. HPLC analysis confirmed the artificial enzyme behavior of PMP complex(Cu) towards the catalytic dephosphorylation of phosphate esters which progressed from ATP to ADP, AMP and, finally, to adenosine. First, PMP complex(Cu) was directly cast on a platinum mesh and used as the electrochemical sensor (Ikeno and Haruyama 2005). Subsequently, the authors changed the biosensor configuration to artificial enzyme-based membranes (Ikeno et al., 2007); and later, they improved the membrane reproducibility by adding polyacrylamide (Ikeno et al., 2009), The membrane-based sensors were able to detect ATP via the electrochemical reduction of the phosphate ions generated in the dephosphorylation reaction (Fig. 5A) (Ikeno et al. 2007, 2009). The product of the catalytic dephosphorylation reaction is PO_4^{3-}, which hardly exists in neutral-pH aqueous solutions since it is

immediately equilibrated to orthophosphate ion form of $H_2PO_4^-$ and HPO_4^{2-}. Both forms of orthophosphate ions are electrochemically stable and do not undergo a redox reaction. Nevertheless, in the case of the artificial enzyme membrane-based biosensor, the reaction product PO_4^{3-} accumulates on the electrode surface and can be electrochemically reduced as shown in the cyclic voltammograms in Fig. 5B, in the presence and in the absence of ATP. The membrane-based systems exhibited response to all biological phosphoric substances (e.g. ATP, GTP, CTP, TTP, ADP, etc). Fig. 5C shows the typical sensor response in which the reduction current increases with the addition of ATP and ADP; however, AMP can only be measure by the sensor at high concentration level.

A synzyme based on acetylcholinesterase (AChE) enzyme was designed by Sgobbi et al. through the modification of polyacrylamide, then used in an electrochemical sensor to quantify organophosphorus pesticides (OPs) (Sgobbi and Machado 2018). A common approach involving the electrochemical detection of pesticides comprises of AChE-based biosensors since AChE activity is inhibited by OPs and carbamate pesticides. The sensing system is based on the direct amperometric detection of thiocholine, the product of the reaction catalyzed by AChE. In the presence of those inhibitors, the amperometric response is decreased and the intensity of inhibition of AChE is proportional to the concentration of pesticide compound. Therefore, the AChE-mimic has to follow two criteria to be applied in electrochemical biosensors: (i) the capacity to catalyze the hydrolysis of acetylthiocholine substrate and (ii) the establishment of interactions with OPs. The mimetic behavior of the modified polyacrylamide (PHA) was scrutinized through theoretical and experimental approaches (Sgobbi et al., 2017). Its mimetic behavior is ascribed to hydroxamic and carboxyl groups inserted along polyacrylamide backbone chain acting as an active site. PHA exhibited significant rate enhancements for acetylthiocholine hydrolysis of over 10^8-fold in pH 7.0 and over 10^7-fold in pH 8.0 compared to spontaneous hydrolysis. Theoretical studies showed a synergetic cooperation between the negatively charged carboxylate groups in the polymer and the positively charged moiety in acetylthiocholine substrate, thus enabling nucleophilic attack by the hydroxamic group. Afterwards, PHA was immobilized on screen printed electrode surface to detect OPs. Fig. 5D shows the working principle of the biomimetic sensor based on modified polyacrylamide. First, the polymer catalyzed the hydrolysis of acetylthiocholine, and then thiocholine is oxidized under an applied potential. Subsequently, the sensor is incubated in OP sample. The catalytic activity of the synzyme was inhibited in the presence of OP and the amperometric response decreased (Fig. 5E). The intensity of inhibition of the modified polyacrylamide activity was proportional to the concentration of OPs. Remarkably, the synzyme activity was not affected by the presence of heavy metals, typical inhibitors of AChE, confirming its superior properties to be used in electrochemical sensing.

More recently, Hryniewicz et al. (2020) demonstrated that an electroactive synzyme based on pyrrole and imidazole copolymers enhanced the degradation of OPs towards heterogeneous catalysis. They showed that polypyrrole did not only act as a matrix to anchor imidazole molecules, but its electroactivity affected the reaction mechanism according to spectroelectrochemical evidence. This outcome revealed a promising synzyme that could be later applied in electrochemical sensing platforms to detect OPs.

Synzymes offer a myriad of possibilities to mimic different enzymes since several types of polymers can be modified with various functional groups. Despite their efficient catalytic performance, they are scarcely used in electrochemical sensors. The reasons behind the limited applications of synzymes in electrochemical sensors are probably associated with challenges to design a new functionalized polymeric system with catalytic activity. The design of a new artificial enzyme involves a certain level of expertise in organic chemistry, concerning the choice of nucleophilic and binding groups to enable efficient catalysis. In comparison to other types of biomimetic materials, such as nanozymes, the synthetic pathways to obtain synzymes may seem to be more complex. However, the selectivity presented by synzyme-based systems is considerably higher, since nanozymes mainly mimic peroxidase enzymes which react with several substrates. Besides, synzymes offer the opportunity to mimic a wide range of enzyme classes, whereas nanozymes mostly mimic oxidoreductases in the context of electrochemical sensing. This is probably related to the tridimensional structures of synzymes which provide a more complex architecture with microenvironments to accommodate the substrate which resembles the enzymatic behavior unlike the simpler nanozymes structures. Another convenience to be considered in synzyme-based sensors is the mitigation of material leaching from electrode surface in comparison to nanozyme-based ones due to the more efficient immobilization of synzymes. Synzyme-based systems open new horizons in biomimetic electrochemical sensors on the account of their high selectivity towards the catalysis of target substrates for detection. Overall, synzymes are a versatile and a promising class of biomimetic materials with high stability to be used in future electrochemical sensing platforms.

5. MIPs – polymers with spatial complementarity

The rise of the so-called molecular imprinted polymers (MIPs) resulted as a distinctive one, introducing a cutting-edge concept for artificially tailored receptors for molecular recognition based on spatial complementarity, or also known as lock-and-key complementarity (Antuña-Jiménez et al., 2012). Traditionally, MIPs can be obtained through a general synthesis route as shown in Fig. 6A (for a more detailed discussion on MIPs synthesis, please refer to the works of (Cormack and Elorza 2004; Vasapollo et al., 2011)).

Briefly, monomers are chosen accordingly to the desired properties of the designed polymer and their affinity with the analyte to be imprinted into the polymeric structure. Once the monomer is chosen, it is introduced to the template molecule, together with the respective cross-linker, in a reaction mixture (Haupt 2001; Haupt and Mosbach 2000). After the reaction is started, the monomers form a complex with the template molecule, which will be stabilized with the formation of a highly cross-linked three-dimensional structure around the template.

The way the template binds to the complementary region in the MIP is fundamentally defined on the formation of the template-monomer complex step, i.e., either covalently or through weaker molecular interactions. Most biological arrangements are of non-covalent nature, resulting essentially from hydrogen bonds, ionic, hydrophobic and van der Waals interactions (Haupt and Mosbach 2000). Employing such features, the non-covalent route confers a greater flexibility of choice regarding the functional monomers and the number of templates that allow for feasible imprinting (Haupt and Mosbach 2000). This attractive adaptability renders the non-covalent approach the most adopted method for the fabrication of MIP-based electrochemical biosensors (Cui et al., 2020; Gui et al., 2018; Radi et al., 2019).

Differently from the non-covalent strategies, the covalent approach relies on the formation of bonds between the functional monomers and the template molecule. The covalent bonding occurs in a pre-polymerization step, which is followed by the development of the template-containing bulk polymer (Haupt 2001; Mayes and Mosbach 1997). To extract the template molecule from the bulk polymer, covalent bonds must be cleaved. Following the cleavage, the reuptake of the analyte might be performed by means of a reversible covalent bonding of the molecule to the memory site in the polymeric structure, or it may be carried out by non-covalent interactions (the latter rebinding mechanism is commonly known as semi-covalent approach) (Algieri et al., 2014; Wulff 2002). Some attractive advantages offered by the covalent approach includes a more homogeneous distribution and a greater density of binding sites, therefore allowing the tuning of specific recognition regions and a higher binding constant during the reuptake of the template. On the other hand, some disadvantages include the need for more aggressive solvents and a more laborious step to remove

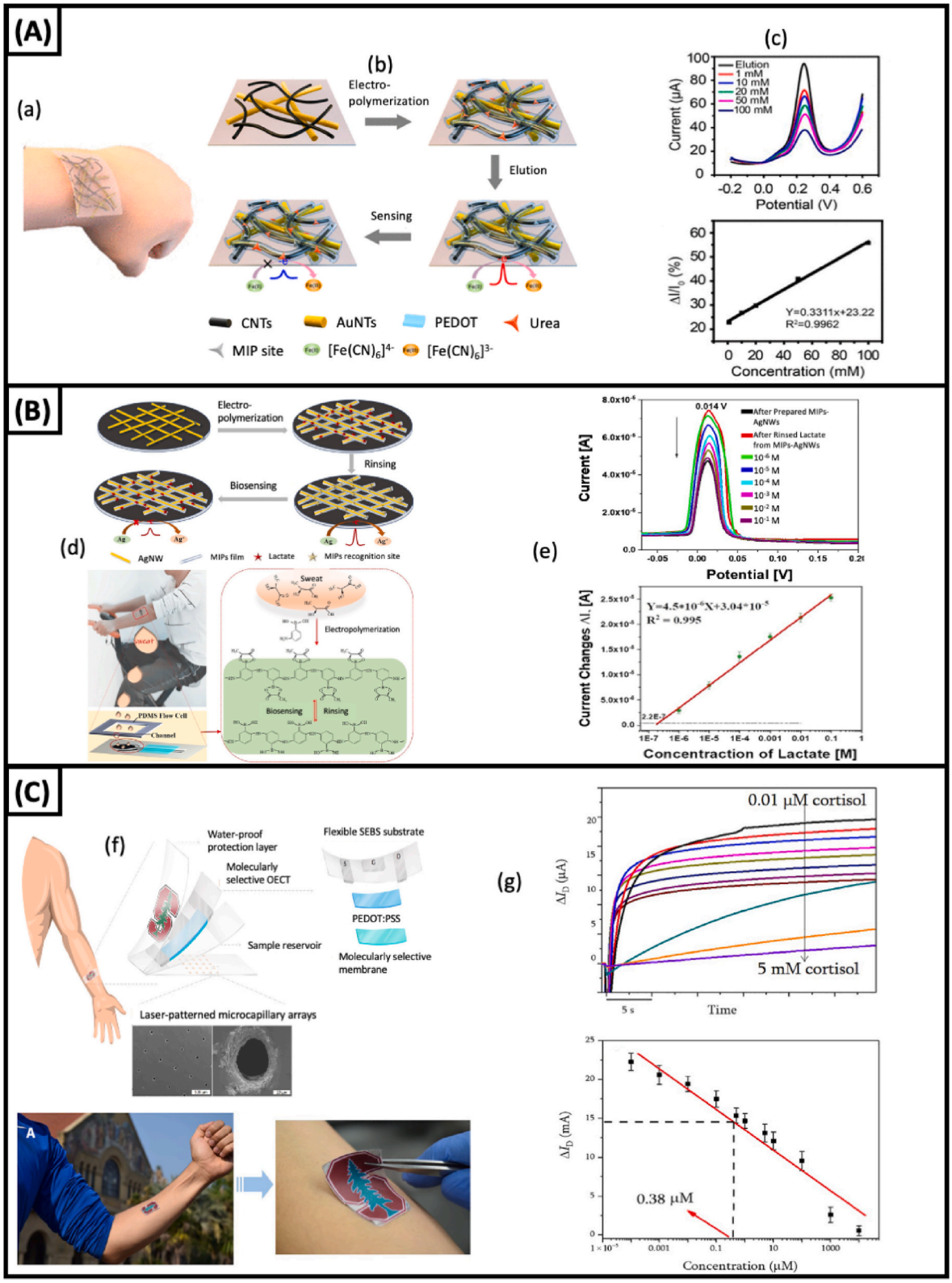

Fig. 7. MIP-based wearable electrochemical biosensors. (A) Wearable device for the detection of sweat urea. (a) and (b) Schematics showing the assembly of the electropolymerized AuNT-CNT-based flexible sensor. (c) Analytical responses of the sensor, reporting analytical curve. Adapted with permission from reference (Liu et al., 2018). (Copyright (2018) American Chemical Society. B) Flexible device for the detection of sweat lactate. (d) Device assembly, showing the steps for the lactate molecule imprinting. (e) Analytical readout of sensor, reporting the acquisition of the analytical curve. Reprinted from reference (Zhang et al., 2020a), Copyright 2020, with permission from Elsevier. (C) Wearable sensor for the detection of sweat cortisol. (f) Assembly of device, along with microscopic structural features. (g) Analytical performance, showing the acquisition of the analytical curve. Adapted from reference (Parlak et al., 2018), Copyright 2018, with permission from American Association for the Advancement of Science.

template molecules after the MIP is obtained (Speltini et al., 2017; Vasapollo et al., 2011).

Although most works today rely on the employment of non-covalent interactions for the fabrication of MIPs, the covalent approach remains at reach in many works, either in fully or semi-covalent strategies. Fig. 6B contrasts, in pairs, the use of the two approaches for the same analyte, employing MIPs as an electrochemical biosensor building piece/analytical tool.

The field of MIP-based electrochemical biosensors has witnessed a very dynamic change in the progress of these devices. Several recent review articles have contributed with different aspects of the latest strategies utilized in the fabrication of MIP-based biomimicking sensors (Beluomini et al., 2019; Cui et al., 2020; Gui et al., 2018; Radi et al., 2019; Yanez-Sedeno et al., 2017; Yang et al., 2018). In terms of electrochemical biosensing, some aspects are of fundamental importance. For that matter, we encourage the reader to take some time and go through the material provided in the Supporting Information that collates some very important aspects regarding the choice of electrode materials in the fabrication of MIP-based electrochemical biosensors and several strategies employed for the integration of MIPs to these platforms.

Regarding analytical assays, MIP-based electrochemical biosensors may benefit from the fact that MIPs can be obtained from virtually any analyte (Ahmad et al., 2019). However, several issues may pose as an obstacle when employing certain molecules as the MIP's template. Such challenges arise when using templates that differ from the target analyte (known as a dummy template), the reason for the choice being cost-related or due to difficulties in the manipulation of the latter (Arak et al., 2019). Consequently, the resulting MIP may present with a lower site specificity and might show signal interference during the analytical assay (Santos et al., 2020). Some other disadvantages that must be considered when choosing to assemble a MIP-based electrochemical biosensor are the right choice of the monomers, which may lead to a considerable non-specific binding if not carefully screened and selected, and the need for the employment of proper quantifying validated methods for the investigation of the removal and rebinding of the target analyte (Verheyen et al., 2011).

Nonetheless, although some recent progress has been charted in the development of unenhanced MIP-based electrochemical sensors (Canfarotta et al., 2018; Naskar et al., 2020; Waffo et al., 2018), most of the latest works have delved into the fabrication of signal-enhanced MIP--based devices in order to tackle some obstacles posed by the use of these polymers. Aside from the use of copolymerization strategies, along with the use of multiple monomers for the MIP preparation, a great deal of attention has been geared towards the employment of nanomaterials to improve both stability and sensitivity of MIP-based biosensors. (Yang et al., 2021).

There are several possibilities to be explored when it comes to nanomaterials for the fabrication of MIP-based biosensors. For instance, the use of metal nanoparticles and carbon nanomaterials have attracted great attention over the last few years. A vastly employed nanomaterial for MIP-based electrochemical biosensors has been gold nanoparticles (Motia et al., 2020; Surya et al., 2020). In addition, recent studies have shown that the combination of different types of nanoparticles may promote a synergetic effect on the catalytic activity and the stability of the biosensor when compared to the isolated nanomaterials. Some of the newest examples of this combination strategy are the fabrication of MIPs that have their activity enhanced through the incorporation of AuPd nanoparticles along with ionic liquids (Yang et al., 2021) (here the presence of the ionic liquid allows for an enhanced nucleation rate of the AuPd NPs), and the combination of metal hydroxides with carbon nanostructures, such as $Ni(OH)_2$ and carbon nanotubes (de Cássia Mendonça et al., 2020). Another strategy that has shown promising results to overcome some disadvantages of MIP-based sensors is the use of magnetic materials for the synthesis of MIPs (Yang et al., 2020). Recent works have contributed to this rising field, showing enhanced stability and recyclability (Afzali et al., 2020; Lu et al., 2021).

Although the stronghold of MIP-based sensors is readily traced to spatial and chemical complementarity, without necessarily mimicking biomolecules, there are several works that have been devoted to showing the biomimetic potential of MIPs for the fabrication of electrochemical biosensors. For instance, glucose electrochemical detection has been studied through multiple methodologies, both using enzymatic and non-enzymatic strategies (Juska and Pemble 2020). Recently, it has been shown that the combination of AuNPs with MIPs enables a highly sensitive biomimetic approach for the non-enzymatic detection of glucose in human serum (Sehit et al., 2020). Some other possibilities that have been dedicated to exploring the ability of MIPs to mimic biomolecules include the development of UV-assisted MIP synthesis for the label-free detection of proteins (mimicking the use of antibodies employed for the same purpose) (Zhao et al., 2019b), the detection of human immunoglobulin G (igG) through a MIP-based platform enhanced with metal-organic frameworks (MOFs) and ionic liquids (mimicking enzyme-linked immunoassays) (Axin Liang et al., 2021), and even the combination of biomolecules, such as DNA, with MIP-based devices enhanced with nanoparticles and carbon nanomaterials (You et al., 2018).

Other than the remarkable new advances that have been proposed in the fabrication of MIP-based electrochemical biosensors, the applications of such devices have been steadily increasing their area of coverage. Table 2 summarizes important information of the latest MIP-based electrochemical biosensors. Among the detection of food (Motia et al., 2021; Pesavento et al., 2021), environmental (Rebelo et al., 2021) and health (Ali et al., 2020; Gao et al., 2021) related analytes, the use of these electrochemical biomimetic platforms for point-of-care (POC) and wearable purposes have gained momentum over the last few years. Once synthetic polymers employed for the fabrication of MIP are highly resilient to fluctuations in both temperature and pressure, this class of biomimetic materials offers interesting advantages for POC and wearable purposes (Parate et al., 2019). Additionally, the electro-polymerization strategy for the incorporation of MIPs into the electrochemical platform offers an important advantage over some other techniques (please, refer to the Supporting Information for a greater detailing on this topic), since it allows for a more homogeneous and controlled MIP deposition. Hence, the latest works dedicated to POC applications have mainly employed electro-polymerization methods along with the addition of signal enhancing materials for the detection of analytes of interest in biofluids, such as sweat and saliva (Diouf et al., 2019; Liu et al., 2018; Parate et al., 2019; Zhang et al. 2019a, 2020a). Fig. 7 displays some strategies employed for the assembly of MIP-based devices aimed at POC and wearable purposes, along with the obtained assay results.

Compared to nanozymes, synzymes and metal complexes, MIP-based electrochemical biosensors offer a very flexible matrix for the choice of target analytes and allow for the fabrication of low-cost devices. On the other hand, due to the inherent imprinting processes, MIPs may promote lower specificity and may require more robust methods to ensure controlled template elution and reuptake steps (Ahmad et al., 2019; Santos et al., 2020). Also, MIPs that display catalytic activity have been shown to promote exciting results in terms of more sensitive and selective electrochemical biomimetic assays (Moretti et al., 2016; Yang et al., 2016b), albeit most of the MIP research is still dedicated to non-catalytic polymeric structures. Finally, in terms of commercial status, MIPs are yet to provide the market with a solid commercialization in the field of biosensors. The main reason for this is due to the still insufficient knowledge and mastery over mass-production of bioassays, differently from enzyme and antibody-based sensors which benefit from a longstanding expertise in industrial scale production of such devices (Lowdon et al., 2020a).

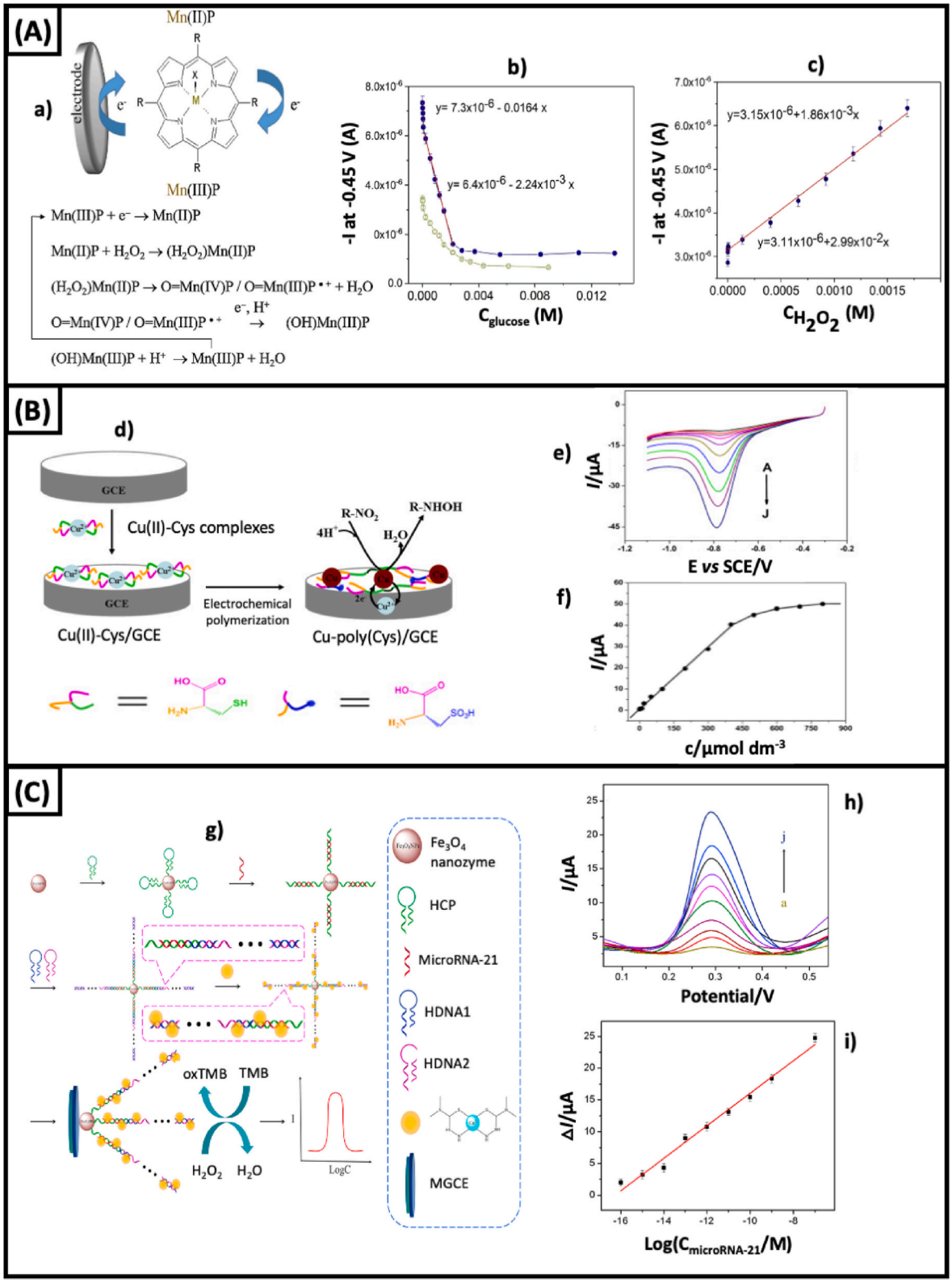

Fig. 8. A) Glassy carbon electrode modified with metal complex based on manganese-porphyrin macrocycles for the detection of serum glucose and H_2O_2. a) Schematics showing H_2O_2 reduction process at the modified electrode. b) and c) Electrochemical readout for the determination of serum glucose and H_2O_2, respectively. Adapted from reference (Peng et al., 2020), Copyright 2020, with permission from Elsevier. B) Glassy carbon electrode modified with copper-cysteine complex for the detection of metronidazole. d) Sensor schematics. e) and f) Analytical performance employing linear sweep stripping voltammetry. Adapted from (Gu et al., 2015), Copyright 2014, with permission from Elsevier. C) Magnetic glassy carbon electrode modified with Fe_3O_4 nanozyme-anchored DNA probes with Cu complex as intercalator for the detection of microRNA-21. g) Sensor assembly. h) and i) Analytical readout employing differential pulse voltammetry. Adapted from (Tian et al., 2018a), Copyright 2018, with permission from Elsevier.

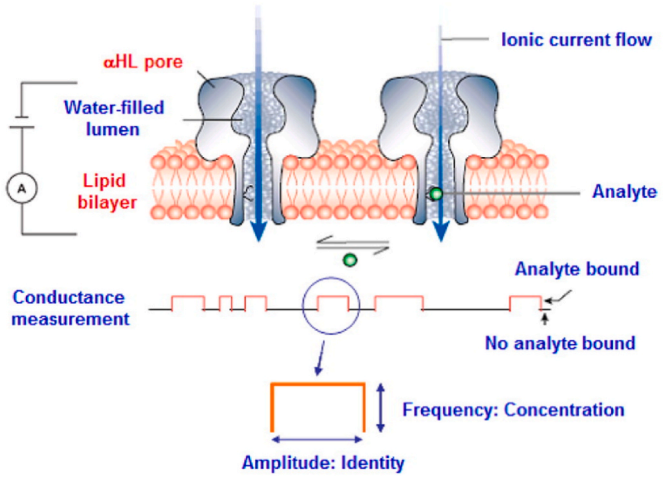

Fig. 9. Stochastic sensing mechanism of nanochannels. The figure illustrates the changes in the electrical conductance measured across a nanochannel built from an engineered α-hemolysin protein inserted in a lipid bilayer membrane. Reprinted with permission from (de la Escosura-Muñiz and Merkoçi 2012). Copyright (2012) American Chemical Society.

6. Metal complexes – coordination materials as enzyme mimics

The usefulness of metal complexes as artificial enzymes becomes apparent when some inherent enzyme characteristics prevent a full manipulation of the biosensing platform, such as high cost and poor stability (Benkovic and Hammes-Schiffer 2003; Cracknell et al., 2008). Hence, metal complexes might come out as a promising enzyme substitute, providing a suitable arrangement of atoms that can give rise to fairly reliable catalytic site mimics. The resulting sensor may undergo a wide experimental setup window, allowing for catalytic site density control and a better electron transfer ratio when compared to some analogous enzyme-based devices (Gascón et al., 2018; Gołębiewski et al., 2019; Huang et al., 2020; Ojani et al., 2012).

The interest in the role of metal complexes as enzyme mimics is not something new. Initially, the major motivation to study these coordination complexes was to provide a deeper understanding of the chemistry of enzymes. Some of the first works to explore the synthesis and characterization of metal complexes as enzyme mimics were after the unravelling of the mechanism of action of dioxygen binding non-heme iron enzymes, especially the role played by iron ions and its ligands (Chiou and Que, 1995; Ha et al., 1995; Kitajima et al., 1990).

There is now a more solid comprehension of the possibilities of metal complexes as artificial enzymes. Some initial obstacles at the time have now been overcome, making way for new challenges. For instance, after the successful synthesis of many oxygenase biomimetic iron complexes, researchers have begun to aim their attention at the proper immobilization of these metal complexes onto nanoparticles, such as gold NPs, seeking to avoid the deactivation of the complex and improve their catalytic reactivity (Sheet et al., 2013).

In the last decade, an assortment of works striving to develop peroxidase mimics with adequate response for sensing applications has been put forth. While many studies focus on the development of iron-based peroxidase mimics (Panda et al., 2011; Zhao et al., 2019c), there are works showing noteworthy progress with different approaches, such as the employment of lanthanide polymerized coordination complexes as peroxidase mimics (Zeng et al., 2016). Although most of these contributions are done in the field of spectroscopic sensors, there are plenty of studies devoted to the development of electrochemical sensors based on metal complex biomimicking chemistry (see Table 2 for some important information on noteworthy recent works covering this topic).

The identity of the metal ion, along with the chosen ligands, is of fundamental importance. Worthy of mention, there has been an extensive assessment on the catalytic activity of oxidase mimicking Cu(II) complexes, wherein several ligands have been analyzed in terms of molecular oxygen assisted oxidation reactions of various organic substrates (Levitzki et al., 1965; Pecht et al., 1967). Drawing from the conclusions of these earlier studies showing that Cu(II) complexation by poly-L-histidine (PLH) rendered the complex with a very close oxidase like ascorbate oxidation kinetics, Wang and collaborators (Wang et al., 2018b) have recently developed a Cu(II)-PLH modified platinum electrode for the detection of Salvianic acid A. To improve the current response, the researchers took advantage of the imidazole groups of PLH to carry out a π-π stacking interaction with carboxylated multi walled carbon nanotubes. As an artificial enzyme structure, this work was able to show a synergetic catalytic effect between the overoxidized imidazole groups from PLH and the redox copper active units.

Another example of the importance of the identity of the ligands, together with their three-dimensional disposition, was investigated by Liao and coworkers (Liao et al., 2019). In this study, aiming at the development of a nitric oxide reductase mimic, the researchers investigated the role of the complex structure in two types of iron porphyrins (planar and picket-fence) for the NO reduction reaction. The assay was carried out by incorporating the porphyrin in ultrathin phospholipid films biomimicking biological cells. As a result, the group was able to unveil some important information on the stepwise electrocatalytic reduction of NO with the picket-fence iron complex. Right after, Huang and collaborators (Huang et al., 2020) reported the fabrication of an iron-based complex modified glassy carbon electrode for the determination of the NO photorelease from sodium nitroprusside. The metal complex was obtained in the form of Fe(II) as central ion with 1,3,5-benzenetricarboxylic acid as ligand, which was electrodeposited onto the electrode surface. The authors reported a Michaelis-Menten behavior for the complex and proposed the oxidation mechanism for NO. Tracking on the influence of ligand substitution, Peng and coworkers (Peng et al., 2020) reported a very thorough investigation on a series of different iron and manganese complexes employing biomimetic porphyrin macrocycles as ligands for the determination of serum H_2O_2 and glucose (see Fig. 8A for the electrochemical sensor assembly schematics and the respective analytical response). Such studies are fundamental for the

Table 3
Selected works of nanochannel-based electrochemical biosensors.

Nanochannel fabrication	Detection strategy	Analyte	Linear range	LOD	Reference
Track-etching on polyimide film	Nanochannel gating	Hg^{2+}	–	8 nM	Tian et al. (2013)
Porous anodized aluminum membrane	Pb^{2+}-Peptide specific at nanochannels walls capture	Pb^{2+}	0.01–0.16 μM 10–100 μM	5 nM	Tu et al. (2021)
Asymmetric track-etching on PET film	Host-guest competition	Adamantanamine	10–1000 nM	4.54 nM	Xie et al. (2020)
Electrochemical anodization followed by etching	Nanochannel gating	Bacterial toxin	Up to 10,000 ng mL^{-1}	1.8 ng mL^{-1}	Reta et al. (2019)
Nanoporous alumina membrane	Nanoconfinement	Ibuprofen	–	0.25 pg/mL	Nagaraj et al. (2014)
Porous anodized aluminum oxide sheet	Glucose-oxidase/peroxidase mimicking catalysis	Glucose	0.5–50 μM	0.2 μM	Xia et al. (2020)
Asymmetric chemical-etching on PET film	Glucose oxidase-modified inner walls catalysis	D-glucose	–	1 nM	Hou et al. (2014)

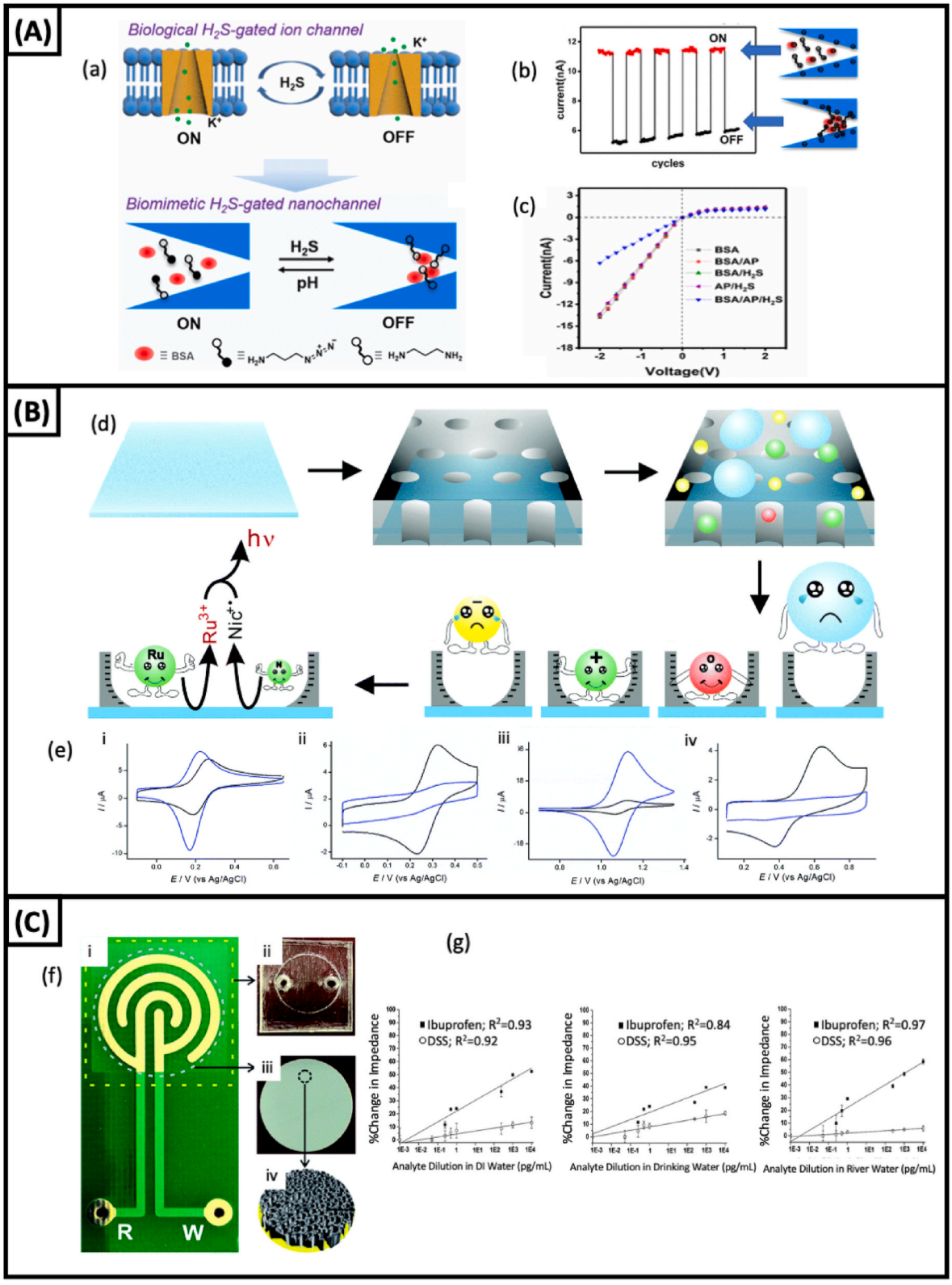

Fig. 10. A) On-Off gating approach with a nanochannel-based biosensor for the detection of H_2S. a) Gating process resulting from the reaction between H_2S and azide groups in the presence of BSA. b) Ionic current response during On-Off cycles. c) K^+, as electrolyte, transport properties in response to the absence and presence of H_2S. Adapted with permission from (Zhang et al., 2019b). Copyright (2019) American Chemical Society. B) ITO electrode modified with nanochannels for the detection of nicotine. d) Disposable silica nanochannels-modified electrode. e) Electrochemical response of the biosensor under the influence of probes of different size and charge: i) FcMeOH, ii) $K_3[Fe(CN)_6]$, iii) $Ru(bpy)_3Cl_2$, iv) rutin. Republished with permission from Royal Society of Chemistry, from (Xiao et al., 2020); permission conveyed through Copyright Clearance Center, Inc. C) Nanochannels employed for the detection of ibuprofen. f) Sensor assembly: i) Gold electrode. ii) PDMS encapsulant for fluid confinement. iii) Nanoporous alumina membrane. iv) Nanochannels. g) Analytical response for, from left to right, ultrapure water, drinking water, river water. Republished with permission from Royal Society of Chemistry, from (Nagaraj et al., 2014); permission conveyed through Copyright Clearance Center, Inc. (For interpretation of the references to color in this figure legend, the reader is referred to the Web version of this article.)

achievement of a better control over the redox properties, the steric interactions and chemical arrangements that occur with the metal complex and its substrate when a biomimetic sensor operates.

One important class of enzymes that is under constant surveillance for the potential development of effective mimicking structures is the peroxidase class. Classically catalyzing the oxidation of organic substrates with the aid of hydrogen peroxide as electron acceptor, this collection of enzymes has seen some major efforts for the synthesis and application of artificial analogous substances. In this sense, Wang and coworkers (Wang et al., 2013) have reported the development of a horseradish peroxidase mimic designed with ferric porphyrin-streptavidin loaded graphene modified glassy carbon electrode, which showed an enhanced peroxidase activity towards the oxidation of o-phenylenediamine in the presence of hydrogen peroxide. The sensor was also combined with a biotinylated molecular beacon in order to obtain a sensitive DNA detection method. A more recent work dealing with peroxidase mimicking chemistry was reported by Brondani and collaborators (Brondani et al., 2017). The researchers developed a copper-based metal-organic framework (MOF) for the determination of catechol in water samples. The electrochemical sensor was obtained by mixing the synthesized Cu-MOF with graphite powder, obtaining a copper based complex modified carbon paste electrode. In this sense, not only can metal complexes be combined with organic frameworks, but they can also be integrated with noble metal nanoparticles, resulting in a tremendous synergistic effect on the electrochemical sensitivity method (Sanghavi et al., 2013; Shu et al., 2015a; Yu et al., 2018). Nonetheless, some simple approaches have shown that a metal complex-based sensor may promote an excellent electrochemical readout without needing to rely on the addition of several enhancing substances. A good example of this strategy is the work reported by Gu and coworkers (Gu et al., 2015), which was able to obtain a promising sensor for the detection of metronidazole by the simple electrodeposition of a copper-poly (cysteine) on the surface of a glassy carbon electrode (check Fig. 8B for sensor assembly and analytical readout).

Although the employment of metal complexes as enzyme mimics aims at the development of sensing platforms not dependent on natural biomolecules, there are situations when the combination of these biomimicking structures with biomolecules, such as DNA and antibodies, may result in attractive benefits; the inclusion of biomolecules may also benefit from the low-cost and high-throughput offered by electrochemical techniques (Tian et al., 2018d). A considerable amount of information has been gathered on the blend of coordination complexes and biomolecules (Ling et al., 2015; Wang et al., 2013; Zhang et al., 2020b), among which one inciting study has recently been reported by Tian and collaborators (Tian et al., 2018a). In this research, as illustrated by Fig. 8C, the authors modified the surface of a magnetic glassy carbon electrode with hairpin capture probes (HCP) anchored on the surface of Fe_3O_4 nanozymes. To attain an enriched signal detection, a Cu(II) complex, employing 4,4-dimethyl-3-thiosemicarbazide as ligand, was used as a planar intercalation molecule, which also allowed for a collaborative catalysis for signal amplification with the immobilized nanozyme. At last, the researchers also employed the catalytic reaction between TMB and hydrogen peroxide to further amplify the electrochemical signal for the detection of microRNA-21. This work appreciably highlights some great advantages of using biomolecules in combination with metal complexes and the possibilities of the synergistic effects that may be harnessed when employing multiple classes of biomimicking materials.

Indeed, the field of metal complexes as biomimicking structures has seen some great changes over the past decade. Many approaches have been put to work, as thoroughly discussed above. However, there are some issues to be attended. In our evaluation, most articles neglect the importance of carrying a meticulous evaluation of the mimicking role of the metal complex. There are very few works which disclose and further elaborate on the catalytic mechanism of the employed complex. Moreover, there is also a lack of a proper comparison between the mimicking complex and the biomolecule which it aims to imitate. Future works should delve deeper into these important aspects. Also, although metal complexes propose to allow more robust assays in terms of stability (when compared to enzymes), this class of biomimetic materials may suffer from dissociation and suboptimal performance when operating in varying analytical environment, such as different pH values. Nonetheless, recent works have shown several strategies to overcome some of these issues, including the incorporation of nanomaterials and/or biomolecules (such as DNA probes). We couldn't find any current progress towards the commercialization of metal complexes-based electrochemical biosensors. Yet, due to the considerable progress in the field over the last decade, we can expect these materials to receive greater protagonism for commercial applications in the near future.

7. Nanochannels – mimics towards stochastic sensing

Another interesting class of biomimetic materials is coined with the name "nanochannels", comprising systems that, differently from nanozymes and biomimetics alike, approach biological selective transport mechanisms. These structures are naturally found in many compartmentalized environments that are kept apart through membranes, such as the ion channels found in most excitable cells (Cornell et al., 1997; Tagliazucchi and Szleifer 2015). The structure of these channels can be of two types, the first being properly known as nanochannels and the second being named nanopores. While the former is defined through the observation of a depth larger than its diameter, the latter is confirmed through a depth shorter than its diameter (diameters commonly fall in the 1–100 nm range). Specifically in this work, we shall deal mostly with nanochannels-based electrochemical biosensors, since this class of materials usually allows for a more selective analyte determination through translocation process (de la Escosura-Muñiz and Merkoçi 2012, 2016; Idley and Stanfield 1996).

Traditionally, a nanochannel may be fabricated through the insertion of a single protein pore into a thin membrane separating two reservoirs of identical composition. The membrane, of hydrophobic nature, might be made of several materials, such as sulfone or Teflon. Then, an orifice (usually 30–100 μm in size) is created in the membrane, across which a lipid bilayer will be formed. The nanochannels itself is created when this lipid bilayer is treated with the addition of a protein solution to the reservoir filled with electrolytes (de la Escosura-Muñiz and Merkoçi 2012, 2016). Pioneering efforts in the insertion of channels into artificial bilayers were achieved with the use of α-hemolysin bacterial protein pores (Albrecht et al., 2010).

In terms of operation, the sensing mechanism yielding an electrical readout can be understood through Fig. 9, which provides an illustration of the so-called stochastic sensing phenomenon. First, a transmembrane potential difference is applied, which in turn alters the ionic flow through the nanochannels. This alteration is translated by the analyte entering the sensing cavity, transiently blocking the previously unperturbed ion current. This current change can be detected with the aid of an electrometer, commonly read as an electrical pulse. The time taken by the analyte to cross the nanochannel extension, along with the amplitude of the pulse, can be employed for the identification of the analyte, while the frequency can be related to the concentration of the analyte (de la Escosura-Muñiz and Merkoçi 2012; Perez Sirkin et al., 2020). For a very thorough coverage over the fundamental aspects of the mechanisms of transport through nanochannels, please refer to the excellent work by Tagliazucchi (Tagliazucchi and Szleifer 2015).

Although for some time the technology of nanochannels and nanopores majorly benefited from the classical fabrication method (artificial bilayer-based), the interest to expand the number of analyte types urged the search for new materials. In this sense, solid-state nanochannels emerged as a very promising alternative, providing the designer with fine dimension and chemical interactivity control (de la Escosura-Muñiz and Merkoçi 2016). Emerging examples for the fabrication of nanochannels comprise graphene (Xu et al., 2013b), hafnium oxide (Shim

et al., 2013), boron nitride (Liu et al., 2013) and molybdenum disulfide (Feng et al., 2015). For solid-state nanochannels, the most common methods employed for fabrication rely on the use of electron-beam lithography, where the ion beam sculpting can be finely tuned through commercial transmission or scanning electron microscopes (de la Escosura-Muñiz and Merkoçi 2016; Romano-Rodríguez and Hernández-Ramírez, 2007).

Regarding applications, nanochannels have now achieved a vast horizon in terms of possibilities, which includes molecular and ionic separation (Wang et al., 2020c), ionic and molecular gating and transport (Chen et al., 2016b; Emilsson et al., 2018), current rectifying (Huang and Hsu 2019; Yen et al., 2020), energy generation (Han et al., 2019; Qian et al., 2020), and DNA sequencing (Howorka and Siwy 2016; Min et al., 2011). In terms of electrochemical biomimetic sensors, nanochannels have also brought forth fruitful advancements through multiple device assembly designs and sensing strategies (see Table 3 for a selection of such works).

Putting into practice the classical methods for the building and operation of nanochannel-based sensors, recent works have shown that it is possible to achieve new possibilities for well-studied glucose biosensors. For instance, a simple 12 μm thick PET substrate can be chemically etched to produce a single nanochannel to be modified at its walls with the anchoring of glucose oxidase enzyme through -COO^- mediated coupling reaction. Once D-glucose is recognized by the nanochannel structure, the enzymatic catalysis takes places and a magnitude and polarity change of the transmembrane ionic current can be measured. This facile method may yield a detection limit as low as 1 nM (Hou et al., 2014). Still aiming at glucose sensing, a recent work by Xia and collaborators (Xia et al., 2020) has reported a solid-state-based biosensor employing the coupling of AuNPs with porous anodized aluminum oxide nanochannels able to detect glucose down to a concentration of 0.2 μM. Strikingly, the authors show that the biomimetic biosensor is able to mimic both glucose oxidase and peroxidase enzymes for the cascade reaction involving glucose, while allowing the device to operate simultaneously through a colorimetric approach and as an electrochemical platform.

Another mechanism of detection that has shown some promising results for biosensing is the gating phenomenon. For instance, the ion-track-etching technique can be employed for the fabrication of nanochannels into PET substrates. The nanochannels can then be used as the medium for the monitoring of the unique reduction reaction between azido groups and H_2S, where the generation of amine groups ensues. The addition of bovine albumin (BSA) allows a direct interaction with the reduced amine groups, resulting in the change of the charge of BSA. Finally, the charged BSA complex gets absorbed by the nanochannel interior walls, inhibiting the ionic current of species such as K^+. Such strategy can be employed for the detection of H_2S with high reversibility and sensor stability (Zhang et al., 2019b) (check Fig. 10A for sensing schematics and the electrical response of the biosensor). Tian and coworkers have also developed a gating-based biosensor for the determination of Hg^{2+} reaching a low limit of detection of 8 nM (Tian et al., 2013), while Reta and collaborators (Reta et al., 2019) have created a porous silicon nanochannel-based electrochemical sensor for the quantification of bacterial toxin through gating strategy yielding a limit of detection of 1.8 ng mL^{-1}.

Size and charge can also be explored for the fabrication of nanochannel-based devices. For instance, disposable silica nanochannels can be grown on top of ITO electrodes, bearing diameters as small as 2 nm. These cavities can then screen among several species, blocking those showing a larger diameter than that of the nanochannel, or/and showing negative charge (see Fig. 10B for some graphical information on this study). The assembled platform may be used as a electrochemiluminescent sensor for the detection of nicotine with a low limit of detection of 27.82 nM (Xiao et al., 2020). Another recent work to explore the selectivity and sensitivity of nanochannel-based electrochemical sensors has been reported by Tu and coworkers (Tu et al., 2021), wherein the authors develop a sensor capable of discriminating among several divalent and trivalent ions, reaching a limit of detection of 5 nM for the detection of Pb^{2+}.

Some other strategies have been shown to result in promising analytical performances. One such approach relies on the use of silica nanoporous membrane-based nanochannels deposited onto gold electrodes. Taking advantage of the small size of molecules such as ibuprofen, an enhanced detection sensitivity can be observed through the nanoconfinement phenomenon. As such, the diffusion of these small species through the nanochannel both improves the mobility of the target analyte to the electrode surface and provides the analyte with more stability and interactivity. The strategy allows for the fabrication of a sensor with a low limit of detection of 0.25 pg/mL for ibuprofen, while showing high selectivity, reliability, low cost and ease of use (check Fig. 10C for some more detailing) (Nagaraj et al., 2014). Employing a yet different approach, Xie and coworkers (Xie et al., 2020) have proposed the detection of adamantanamine with the employment of nanochannels fabricated on PET films and subsequently modified with p-toluidine and assembled with cucurbit [7]uril (CB [7]). If present, the target analyte undergoes a host-guest substitution competition with the p-toluidine-CB [7] complex, resulting in the hydrophobicity of the nanochannels and, consequently, a disturbance in the ionic current. This strategy allowed the device to reach a limit of detection of 4.54 nM for the quantification of adamantanamine.

As discussed, nanochannels form a class of biomimetic materials with great versatility for several applications, showing especially successful and promising results for the fabrication and operation of electrochemical biosensors. Although nanochannels have achieved commercialization for some applications, particularly for DNA sequencing (Howorka and Siwy 2016; Perez Sirkin et al., 2020), there's still a progress lack in terms of electrochemical biomimetic sensors. Nonetheless, as we have covered, these biomimetic structures offer great tunable features that may promote laboratory-based platforms for a larger production scale in the coming years. However, when comparing nanochannels to the other classes of biomimetic materials, there are some differences worth noting. Generally, nanochannels need more precision-controlled synthesis, either through the use of external expensive devices (such as electron microscopes) or through wet chemistry route. Consequently, sensors made this way are substantially more time and resource consuming. Moreover, a current challenge to be overcome in order for such materials to reach commercial status is the need for the integration of nanochannels into chemical networks, allowing the devices to sense a spectrum of analytes simultaneously.

8. Perspectives and conclusions

The field of biomimetic materials offer a myriad of exciting possibilities to mimic natural enzymes or biological systems using MIPs, synzymes, nanozymes, nanochannels and metal complexes. From simple 1D/2D structures to complex tridimensional architectures, outstanding catalytic performances can be achieved through surface atoms (nanozymes) or via an intricate macrostructure with cavities and tailored functional groups (synzymes and MIPs). In some circumstances, superior kinetic performance is reached in comparison to natural enzymes; however, the reaction rate is not the only parameter pursued when assessing a mimicking system. Attention must be given to selectivity and specificity as well, since these criteria are the shortcomings of most artificial enzymes. In the case of nanozymes, some challenges still need to be addressed to enable their use in commercial sensors. In case, a proper evaluation of their reproducibility and functional lifetime are both affected by physical (size, shape, porosity) and chemical (surface functional groups) attributes, but also of their long-term stability in physiological conditions. Regarding macrostructures with enzyme-like activity (MIPs and synzymes), their long-term stability is also a critical issue for commercial devices as well as the more complicated synthesis pathways required for these materials. On the other hand, it is possible

to achieve enhanced selectivity with these biomimetic systems due to cavities similar to the active site in natural enzymes, and different possibilities of chemical functionalization to allow user-defined catalytic activities. Selectivity enhancements can be achieved by fine-tuning the chemical groups inserted in polymeric structures, like synzymes; or changing the ligands or metallic ions in complexes, for example. The horizons in Biomimetic Chemistry may go through continuous research on new materials with large surface area, active sites, cooperative reaction groups (binding groups and catalytic groups) aiming for more efficient and stable systems. Meanwhile, nanochannel-based systems offer interesting and versatile approaches, but they involve more complicated synthesis routes demanding high controlled conditions to achieve well-organized structures. Additionally, biofouling is a critical issue involving market applications of these biomimetic materials integrated into electrochemical sensing platforms. Since the electrodes are in direct contact with complex matrices to perform the desired analysis, many different species may adsorb on the electrode surface affecting sensor reproducibility. Biofouling is not an exclusive problematic for biomimetic electrochemical sensors, as enzymatic-based ones also undergo the same situation, demanding continuous efforts to overcome it.

From the technological perspective, one of the main challenges is the gap between the innovative concepts brought by academic research and its integration with the market needs, towards validation procedures, inaccessibility of biological samples, known as real-world samples, and limited experience on marketable devices. A plausible solution could be attained by the collaboration among academies and industries to fulfill the necessities of more robust, stable and low-cost sensors.

Declaration of competing interest

The authors declare that they have no known competing financial interests or personal relationships that could have appeared to influence the work reported in this paper.

Acknowledgements

The authors are thankful to the Coordenação de Aperfeiçoamento de Pessoal de Nível Superior (CAPES - Finance code 001), Conselho Nacional de Desenvolvimento Científico e Tecnológico (CNPq) and Fundação de Amparo à Pesquisa do Estado de São Paulo (FAPESP Proc. 2015/26651-3, 2016/01919-6 and 2019/01777-5).

Appendix A. Supplementary data

Supplementary data to this article can be found online at https://doi.org/10.1016/j.bios.2021.113242.

References

Afzali, M., Mostafavi, A., Shamspur, T., 2020. Arab. J. Chem. 13 (8), 6626–6638.
Ahmad, O.S., Bedwell, T.S., Esen, C., Garcia-Cruz, A., Piletsky, S.A., 2019. Trends Biotechnol. 37 (3), 294–309.
Albrecht, T., Edel, J.B., Winterhalter, M., 2010. J. Phys. Condens. Matter 22 (45), 450301.
Algieri, C., Drioli, E., Guzzo, L., Donato, L., 2014. Sensors 14 (8), 13863–13912.
Ali, M.R., Bacchu, M.S., Daizy, M., Tarafder, C., Hossain, M.S., Rahman, M.M., Khan, M. Z.H., 2020. Anal. Chim. Acta 1121, 11–16.
Alizadeh, N., Salimi, A., 2021. J. Nanobiotechnol. 19 (1), 26.
Alizadeh, N., Salimi, A., Sham, T.-K., Bazylewski, P., Fanchini, G., 2020. ACS Omega 5 (21), 11883–11894.
Andrianantoandro, E., Basu, S., Karig, D.K., Weiss, R., 2006. Mol. Syst. Biol. 2.
Anjalidevi, C., Dharuman, V., Shankara Narayanan, J., 2013. Sensor. Actuator. B Chem. 182, 256–263.
Antonacci, A., Arduini, F., Moscone, D., Palleschi, G., Scognamiglio, V., 2016. Chapter 10 - commercially available (Bio)sensors in the agrifood sector. In: Scognamiglio, V., Rea, G., Arduini, F., Palleschi, G. (Eds.), Comprehensive Analytical Chemistry. Elsevier, pp. 315–340.
Antuña-Jiménez, D., Díaz-Díaz, G., Blanco-López, M.C., Lobo-Castañón, M.J., Miranda-Ordieres, A.J., Tuñón-Blanco, P., 2012. Molecularly imprinted electrochemical sensors: past, present, and future. In: Li, S., Ge, Y., Piletsky, S.A., Lunec, J. (Eds.), Molecularly Imprinted Sensors. Elsevier, pp. 1–34.
Arak, H., Karimi Torshizi, M.A., Hedayati, M., Rahimi, S., 2019. Toxicon 166, 66–75.
Arduini, F., Cinti, S., Scognamiglio, V., Moscone, D., Palleschi, G., 2017. Anal. Chim. Acta 959, 15–42.
Arduini, F., Micheli, L., Moscone, D., Palleschi, G., Piermarini, S., Ricci, F., Volpe, G., 2016. Trac. Trends Anal. Chem. 79, 114–126.
Asati, A., Santra, S., Kaittanis, C., Nath, S., Perez, J.M., 2009. Angew. Chem. Int. Ed. 48 (13), 2308–2312.
Avenier, F., Domingos, J.B., Van Vliet, L.D., Hollfelder, F., 2007. J. Am. Chem. Soc. 129 (24), 7611–7619.
Avenier, F., Hollfelder, F., 2009. Chem. Eur J. 15 (45), 12371–12380.
Axin Liang, A., Huipeng Hou, B., Shanshan Tang, C., Liquan Sun, D., Aiqin Luo, E., 2021. Bioelectrochemistry 137 107671.
Bahadır, E.B., Sezgintürk, M.K., 2015. Anal. Biochem. 478, 107–120.
Baldim, V., Bedioui, F., Mignet, N., Margaill, I., Berret, J.F., 2018. Nanoscale 10 (15), 6971–6980.
Beltrame, P., Comotti, M., Della Pina, C., Rossi, M., 2006. Appl. Catal. Gen. 297 (1), 1–7.
Beluomini, M.A., da Silva, J.L., de Sá, A.C., Buffon, E., Pereira, T.C., Stradiotto, N.R., 2019. J. Electroanal. Chem. 840, 343–366.
Benkovic, S.J., Hammes-Schiffer, S., 2003. Science 301 (5637), 1196–1202.
Bhattacharjee, R., Tanaka, S., Moriam, S., Masud, M.K., Lin, J., Alshehri, S.M., Ahamad, T., Salunkhe, R.R., Nguyen, N.-T., Yamauchi, Y., Hossain, M.S.A., Shiddiky, M.J.A., 2018. J. Mater. Chem. B 6 (29), 4783–4791.
Biella, S., Castiglioni, G.L., Fumagalli, C., Prati, L., Rossi, M., 2002a. Catal. Today 72 (1–2), 43–49.
Biella, S., Prati, L., Rossi, M., 2002b. J. Catal. 206 (2), 242–247.
Breslow, R., 1972. Chem. Soc. Rev. 1 (4), 553–580.
Breslow, R., 1980. Acc. Chem. Res. 13 (6), 170–177.
Breslow, R., 1982. Science 218 (4572), 532–537.
Breslow, R., 1995. Acc. Chem. Res. 28 (3), 146–153.
Breslow, R., 2005. Artificial Enzymes. Wiley-VCH, Weinheim.
Brondani, D., Zapp, E., daSilvaHeying, R., deSouza, B., CruzVieira, I., 2017. Electroanalysis 29 (12), 2810–2817.
Cai, X., Gao, Q., Zuo, S., Zhao, H., Lan, M., 2020. Electroanalysis 32 (3), 598–605.
Cai, X., Shi, L., Sun, W., Zhao, H., Li, H., He, H., Lan, M., 2018. Biosens. Bioelectron. 102, 171–178.
Campuzano, S., Pedrero, M., Yáñez-Sedeño, P., Pingarrón, J.M., 2020. Microchim. Acta 187 (8), 423.
Canfarotta, F., Czulak, J., Guerreiro, A., Cruz, A.G., Piletsky, S., Bergdahl, G.E., Hedstrom, M., Mattiasson, B., 2018. Biosens. Bioelectron. 120, 108–114.
Chatterjee, B., Das, S.J., Anand, A., Sharma, T.K., 2020. Mater. Sci. Energy Technol. 3, 127–135.
Chen, D., Wang, D., Hu, X., Long, G., Zhang, Y., Zhou, L., 2019. Sensor. Actuator. B Chem. 296, 126650.
Chen, L., Sha, L., Qiu, Y., Wang, G., Jiang, H., Zhang, X., 2015. Nanoscale 7 (7), 3300–3308.
Chen, L., Wang, X., Lu, W., Wu, X., Li, J., 2016a. Chem. Soc. Rev. 45 (8), 2137–2211.
Chen, Y., Zhou, D., Meng, Z., Zhai, J., 2016b. Chem. Commun. 52 (65), 10020–10023.
Chen, Z., Yin, J.-J., Zhou, Y.-T., Zhang, Y., Song, L., Song, M., Hu, S., Gu, N., 2012. ACS Nano 6 (5), 4001–4012.
Chevalier, Y., LockToyKi, Y., leNouen, D., Mahy, J.P., Goddard, J.P., Avenier, F., 2018. Angew. Chem. Int. Ed. 57 (50), 16412–16415.
Chiou, Y.M., Que Jr., L., 1995. J. Am. Chem. Soc. 117 (14), 3999–4013.
Cho, I.H., Kim, D.H., Park, S., 2020. Biomater. Res. 24 (1), 6.
Cieplak, M., Szwabinska, K., Sosnowska, M., Chandra, B.K., Borowicz, P., Noworyta, K., D'Souza, F., Kutner, W., 2015. Biosens. Bioelectron. 74, 960–966.
Comotti, M., Della Pina, C., Matarrese, R., Rossi, M., 2004. Angew. Chem. Int. Ed. 43 (43), 5812–5815.
Cormack, P.A., Elorza, A.Z., 2004. J. Chromatogr. B Analyt Technol. Biomed. Life Sci. 804 (1), 173–182.
Cornell, B., Braach-Maksvytis, V., King, L., Osman, P.D.J., Raguse, B., Wieczorek, L., Pace, R.J., 1997. Nature 387, 580–583.
Cracknell, J.A., Vincent, K.A., Armstrong, F.A., 2008. Chem. Rev. 108 (7), 2439–2461.
Cui, F., Zhou, Z., Zhou, H.S., 2020. Sensors 20 (4).
Cui, Z., Wu, D., Zhang, Y., Ma, H., Li, H., Du, B., Wei, Q., Ju, H., 2014. Anal. Chim. Acta 807, 44–50.
Das, M., Patil, S., Bhargava, N., Kang, J.F., Riedel, L.M., Seal, S., Hickman, J.J., 2007. Biomaterials 28 (10), 1918–1925.
Das, R., Dhiman, A., Kapil, A., Bansal, V., Sharma, T.K., 2019. Anal. Bioanal. Chem. 411 (6), 1229–1238.
Dashtestani, F., Ghourchian, H., Eskandari, K., Rafiee-Pour, H.-A., 2015. Microchim. Acta 182 (5), 1045–1053.
de Cássia Mendonça, J., da Rocha, L.R., Capelari, T.B., Prete, M.C., Angelis, P.N., Segatelli, M.G., Tarley, C.R.T., 2020. J. Electroanal. Chem. 878.
de la Escosura-Muñiz, A., Merkoçi, A., 2012. ACS Nano 6 (9), 7556–7583.
de la Escosura-Muñiz, A., Merkoçi, A., 2016. Trac. Trends Anal. Chem. 79, 134–150.
Dedeoglu, A., Kaya, S.I., Bakirhan, N.K., Ozkan, S.A., 2020. Chapter Twelve - Nanotechnological approaches and materials in commercial biosensors. In: Sezgintürk, M.K. (Ed.), Commercial Biosensors and Their Applications. Elsevier, pp. 301–353.
Dhull, V., Gahlaut, A., Dilbaghi, N., Hooda, V., 2013. Biochem. Res. Int. 2013, 731501, 731501.
Diouf, A., Bouchikhi, B., El Bari, N., 2019. Mater. Sci. Eng. C Mater. Biol. Appl. 98, 1196–1209.
Dong, Z., Luo, Q., Liu, J., 2012. Chem. Soc. Rev. 41 (23), 7890–7908.
Dutta, A.K., Maji, S.K., Srivastava, D.N., Mondal, A., Biswas, P., Paul, P., Adhikary, B., 2012. ACS Appl. Mater. Interfaces 4 (4), 1919–1927.

El Harrad, L., Bourais, I., Mohammadi, H., Amine, A., 2018. Sensors 18 (1), 164.
El-Gewely, M.R., 2003. Biotechnology Annual Review. Elsevier Science, Amsterdam.
Emilsson, G., Sakiyama, Y., Malekian, B., Xiong, K., Adali-Kaya, Z., Lim, R.Y.H., Dahlin, A.B., 2018. ACS Cent. Sci. 4 (8), 1007–1014.
Fan, K., Wang, H., Xi, J., Liu, Q., Meng, X., Duan, D., Gao, L., Yan, X., 2016. Chem. Commun. 53 (2), 424–427.
Fan, K., Wang, H., Xi, J., Liu, Q., Meng, X., Duan, D., Gao, L., Yan, X., 2017. Chem. Commun. 53 (2), 424–427.
Feng, J., Liu, K., Graf, M., Lihter, M., Bulushev, R.D., Dumcenco, D., Alexander, D.T., Krasnozhon, D., Vuletic, T., Kis, A., Radenovic, A., 2015. Nano Lett. 15 (5), 3431–3438.
Feng, X., Li, X., Shi, H., Huang, H., Wu, X., Song, W., 2014. Anal. Chim. Acta 852, 37–44.
Ferreira, J.G.L., Grein-Iankovski, A., Oliveira, M.A.S., Simas-Tosin, F.F., Riegel-Vidotti, I. C., Orth, E.S., 2015a. Chem. Commun. 51 (28), 6210–6213.
Ferreira, J.G.L., Ramos, L.M., de Oliveira, A.L., Orth, E.S., Neto, B.A.D., 2015b. J. Org. Chem. 80 (11), 5979–5983.
Gallay, P., Eguílaz, M., Rivas, G., 2020. Biosens. Bioelectron. 148, 111764.
Gao, B., Liang, Z., Han, D., Han, F., Fu, W., Wang, W., Liu, Z., Niu, L., 2021. Talanta 224, 121924.
Gao, L., Fan, K., Yan, X., 2017. Theranostics 7 (13), 3207–3227.
Gao, L., Zhuang, J., Nie, L., Zhang, J., Zhang, Y., Gu, N., Wang, T., Feng, J., Yang, D., Perrett, S., Yan, X., 2007. Nat. Nanotechnol. 2 (9), 577–583.
Gascón, V., Jiménez, M.B., Blanco, R.M., Sanchez-Sanchez, M., 2018. Catal. Today 304, 119–126.
Gayda, G.Z., Demkiv, O.M., Gurianov, Y., Serkiz, R.Y., Gonchar, M.V., Nisnevitch, M., 2020. Proceedings 60 (1), 58.
Gibson, T.D., 1999. Analusis 27 (7), 630–638.
Gobbo, P., Tian, L.F., Kumar, B., Turvey, S., Cattelan, M., Patil, A.J., Carraro, M., Bonchio, M., Mann, S., 2020. Nat. Commun. 11 (1).
Gołębiewski, P., Puciłowski, B., Sommer, F., Kubik, S., Daniels, M., Dehaen, W., Sivasankaran, U., Kumar, K.G., Radecka, H., Radecki, J., 2019. Sensor. Actuator. B Chem. 285, 536–545.
Gooding, J.J., 2019. ACS Sens. 4 (9), 2213–2214.
Gu, Y., Yan, X., Liu, W., Li, C., Chen, R., Tang, L., Zhang, Z., Yang, M., 2015. Electrochim. Acta 152, 108–116.
Gui, R., Jin, H., Guo, H., Wang, Z., 2018. Biosens. Bioelectron. 100, 56–70.
Guivar, J.A.R., Fernandes, E.G.R., Zucolotto, V., 2015. Talanta 141, 307–314.
Gumerova, N.I., Rompel, A., 2020. Chem. Soc. Rev. 49 (21), 7568–7601.
Guo, S., Guo, L., 2019. J. Phys. Chem. C 123 (50), 30318–30334.
Ha, E.H., Ho, R.Y.N., Kisiel, J.F., Valentine, J.S., 1995. Inorg. Chem. 34 (9), 2265–2266.
Haimov, A., Cohen, H., Neumann, R., 2004. J. Am. Chem. Soc. 126 (38), 11762–11763.
Han, J., Bae, C., Chae, S., Choi, D., Lee, S., Nam, Y., Lee, C., 2019. Electrochim. Acta 319, 366–374.
Haupt, K., 2001. Analyst 126 (6), 747–756.
Haupt, K., Mosbach, K., 2000. Chem. Rev. 100 (7).
He, Q., Cui, Y., Li, J., 2009. Chem. Soc. Rev. 38 (8), 2292–2303.
Ho, M.Y.K., Rechnitz, G.A., 1987. Anal. Chem. 59 (3), 536–537.
Hou, G., Zhang, H., Xie, G., Xiao, K., Wen, L., Li, S., Tian, Y., Jiang, L., 2014. J. Mater. Chem. 2 (45), 19131–19135.
Howorka, S., Siwy, Z., 2016. ACS Nano 10 (11), 9768–9771.
Hryniewicz, B.M., Wolfart, F., Gómez-Romero, P., Orth, E.S., Vidotti, M., 2020. Electrochim. Acta 338, 135842.
Hu, X., Chen, J., Hu, R., Zhu, Z., Lai, Z., Zhu, X., Zhu, H., Koh, K., Chen, H., 2021. Sensor. Actuator. B Chem. 333, 129564.
Hu, X., Wu, X., Yang, F., Wang, Q., He, C., Liu, S., 2016. Talanta 148, 29–36.
Huang, L., Sun, D.-W., Pu, H., Wei, Q., 2019a. Compr. Rev. Food Sci. Food Saf. 18 (5), 1496–1513.
Huang, L., Zhang, W., Chen, K., Zhu, W., Liu, X., Wang, R., Zhang, X., Hu, N., Suo, Y., Wang, J., 2017. Chem. Eng. J. 330, 746–752.
Huang, P., Zhang, B., Dang, X., Chen, H., Zheng, D., 2020. J. Electroanal. Chem. 860.
Huang, W.C., Hsu, J.P., 2019. J. Colloid Interface Sci. 557, 683–690.
Huang, Y., Ren, J., Qu, X., 2019b. Chem. Rev. 119 (6), 4357–4412.
Hwang, D.W., Lee, S., Seo, M., Chung, T.D., 2018. Anal. Chim. Acta 1033, 1–34.
Idley, D.J., Stanfield, P.R., 1996. Ion Channels: Molecules in Action. Cambridge University Press, New York.
Ikeno, S., Asakawa, H., Haruyama, T., 2007. Anal. Chem. 79 (15), 5540–5546.
Ikeno, S., Haruyama, T., 2005. Sensor. Actuator. B Chem. 108 (1), 608–612.
Ikeno, S., Yoshida, T., Haruyama, T., 2009. Analyst 134 (2), 337–342.
Jiang, D., Ni, D., Rosenkrans, Z.T., Huang, P., Yan, X., Cai, W., 2019. Chem. Soc. Rev. 48 (14), 3683–3704.
Juska, V.B., Pemble, M.E., 2020. Sensors 20 (21).
Kang, K., Wang, B.B., Ji, X.P., Liu, Y.H., Zhao, W.R., Du, Y.Q., Guo, Z.Y., Ren, J.J., 2021. RSC Adv. 11 (4), 2446–2452.
Kim, D.M., Moon, J.M., Lee, W.C., Yoon, J.H., Choi, C.S., Shim, Y.B., 2017. Biosens. Bioelectron. 91, 276–283.
Kim, M.S., Cho, S., Joo, S.H., Lee, J., Kwak, S.K., Kim, M.I., Lee, J., 2019a. ACS Nano 13 (4), 4312–4321.
Kim, M.S., Lee, J., Kim, H.S., Cho, A., Shim, K.H., Le, T.N., An, S.S.A., Han, J.W., Kim, M. I., Lee, J., 2019b. Adv. Funct. Mater. 30 (1).
Kirby, A.J., Hollfelder, F., 2009. From Enzyme Models to Model Enzymes. Springer, Cambridge.
Kitajima, N., Fukui, H., Morooka, Y., Mizutani, Y., Kitagawa, T., 1990. J. Am. Chem. Soc. 112 (17), 6402–6403.
Klotz, I.M., Royer, G.P., Scarpa, I.S., 1971. Proc. Natl. Acad. Sci. Unit. States Am. 68 (2), 263–264.
Ko, E., Tran, V.-K., Son, S.E., Hur, W., Choi, H., Seong, G.H., 2019. Sensor. Actuator. B Chem. 294, 166–176.
Kong, W., Guo, X., Jing, M., Qu, F., Lu, L., 2020. Biosens. Bioelectron. 150, 111875.
Koyappayil, A., Berchmans, S., Lee, M.-H., 2020. Colloids Surf. B Biointerfaces 189, 110840.
Koyappayil, A., Lee, M.-H., 2021. Sensors 21 (1), 89.
Kuah, E., Toh, S., Yee, J., Ma, Q., Gao, Z., 2016. Chem. Eur J. 22 (25), 8404–8430.
Kurbanoglu, S., Ozkan, S.A., Merkoçi, A., 2017. Biosens. Bioelectron. 89, 886–898.
Lefever, R., Goldbeter, A., 1978. Molecular Movements and Chemical Reactivity as Conditioned by Membranes, Enzymes and Other Macromolecules: XVIth Solvay Conference on Chemistry. Wiley-Interscience, New York.
Levitzki, A., Pecht, I., Anbar, M., 1965. Nature 207, 1386–1387.
Li, S., Ma, X., Pang, C., Wang, M., Yin, G., Xu, Z., Li, J., Luo, J., 2021. Biosens. Bioelectron. 176, 112944.
Li, W., Fan, G.-C., Gao, F., Cui, Y., Wang, W., Luo, X., 2019a. Biosens. Bioelectron. 127, 64–71.
Li, X., Li, X., Li, D., Zhao, M., Wu, H., Shen, B., Liu, P., Ding, S., 2020. Biosens. Bioelectron. 168, 112554.
Li, X., Wang, L.J., Du, D., Ni, L., Pan, J.M., Niu, X.H., 2019b. Trac. Trends Anal. Chem. 120.
Li, Y., Shi, L., Cai, X., Zhao, H., Niu, X., Lan, M., 2019c. Electrochim. Acta 294, 304–311.
Liang, M., Yan, X., 2019. Acc. Chem. Res. 52 (8), 2190–2200.
Liao, X., Zhang, L., Wang, S., Lei, J., 2019. Electrochem. Commun. 100, 60–63.
Ling, P., Lei, J., Zhang, L., Ju, H., 2015. Anal. Chem. 87 (7), 3957–3963.
Ling, P., Qian, C., Yu, J., Gao, F., 2020. Biosens. Bioelectron. 149, 111838.
Liu, B., Liu, J., 2017. Nano Res. 10 (4), 1125–1148.
Liu, J., Zhang, W., Peng, M., Ren, G., Guan, L., Li, K., Lin, Y., 2020. ACS Appl. Mater. Interfaces 12 (26), 29631–29640.
Liu, J.W., 2019. J. Anal. Test. 3 (3), 189–190.
Liu, L., Du, J., Liu, W.-e., Guo, Y., Wu, G., Qi, W., Lu, X., 2019a. Anal. Bioanal. Chem. 411 (10), 2189–2200.
Liu, L., Zhao, H., Shi, L., Lan, M., Zhang, H., Yu, C., 2017. Electrochim. Acta 227, 69–76.
Liu, N., Xu, Z., Morrin, A., Luo, X., 2019b. Anal. Methods 11 (6), 702–711.
Liu, S., Lu, B., Zhao, Q., Li, J., Gao, T., Chen, Y., Zhang, Y., Liu, Z., Fan, Z., Yang, F., You, L., Yu, D., 2013. Adv. Mater. 25 (33), 4549–4554.
Liu, T., Niu, X., Shi, L., Zhu, X., Zhao, H., Lana, M., 2015. Electrochim. Acta 176, 1280–1287.
Liu, W., Yang, H., Ma, C., Ding, Y.-n., Ge, S., Yu, J., Yan, M., 2014. Anal. Chim. Acta 852, 181–188.
Liu, Y.L., Liu, R., Qin, Y., Qiu, Q.F., Chen, Z., Cheng, S.B., Huang, W.H., 2018. Anal. Chem. 90 (21), 13081–13087.
Lowdon, J.W., Dilien, H., Singla, P., Peeters, M., Cleij, T.J., van Grinsven, B., Eersels, K., 2020a. Sensor. Actuator. B Chem. 325, 128973.
Lowdon, J.W., Dilien, H., Singla, P., Peeters, M., Cleij, T.J., van Grinsven, B., Eersels, K., 2020b. Sens. Actuator. B-Chem. 325.
Lu, J., Hu, Y., Wang, P., Liu, P., Chen, Z., Sun, D., 2020. Sensor. Actuator. B: Chemical 311, 127909.
Lu, Y.C., Xiao, W.W., Wang, J.Y., Xiong, X.H., 2021. Anal. Bioanal. Chem. 413 (2), 389–401.
Luong, J.H.T., Male, K.B., Glennon, J.D., 2008. Biotechnol. Adv. 26 (5), 492–500.
Luque de Castro, M.D., Herrera, M.C., 2003. Biosens. Bioelectron. 18 (2–3), 279–294.
Lv, H., Li, Y., Zhang, X., Gao, Z., Zhang, C., Zhang, S., Dong, Y., 2018. Biosens. Bioelectron. 112, 1–7.
Machini, W.B., Teixeira, M.F., 2016. Biosens. Bioelectron. 79, 442–448.
Mahmudunnabi, R.G., Farhana, F.Z., Kashaninejad, N., Firoz, S.H., Shim, Y.-B., Shiddiky, M.J.A., 2020. Analyst 145 (13), 4398–4420.
Majdinasab, M., Yaqub, M., Rahim, A., Catanante, G., Hayat, A., Marty, J.L., 2017. Sensors 17 (9), 1947.
Manea, F., Houillon, F.B., Pasquato, L., Scrimin, P., 2004. Angew. Chem. Int. Ed. 43 (45), 6165–6169.
Marchetti, L., Levine, M., 2011. ACS Catal. 1 (9), 1090–1118.
Matos-Peralta, Y., Antuch, M., 2019. J. Electrochem. Soc. 167 (3), 037510.
Mayes, A.G., Mosbach, K., 1997. Trac. Trends Anal. Chem. 16 (6), 321–332.
Mazzocchi, R.A., 2016. ACS Sens. 1 (10), 1167–1170.
Min, S., Kim, W., Cho, Y., 2011. Nat. Nanotechnol. 6, 162–165.
Mohan, A.M.V., Rajendran, V., Mishra, R.K., Jayaraman, M., 2020. TrAC Trends Anal. Chem. (Reference Ed.) 131, 116024.
Monteiro, T., Almeida, M.G., 2019. Crit. Rev. Anal. Chem. 49 (1), 44–66.
Moretti, E.d.S., de Fátima Giarola, J., Kuceki, M., Prete, M.C., Pereira, A.C., Teixeira Tarley, C.R., 2016. RSC Adv. 6 (34), 28751–28760.
Motia, S., Bouchikhi, B., El Bari, N., 2021. Talanta 223 (Pt 1), 121689.
Motia, S., Bouchikhi, B., Llobet, E., El Bari, N., 2020. Talanta 216, 120953.
Mu, J., Zhang, L., Zhao, M., Wang, Y., 2013. J. Mol. Catal. Chem. 378, 30–37.
Nagaraj, V.J., Jacobs, M., Vattipalli, K.M., Annam, V.P., Prasad, S., 2014. Environ. Sci. Process Impacts 16 (1), 135–140.
Naskar, H., Ghatak, B., Biswas, S., Singh, P.P., Tudu, B., Bandyopadhyay, R., 2020. IEEE Sensor. J. 20 (1), 39–46.
Ndunda, E.N., 2020. J. Mol. Recogn. 33 (11), e2855.
Neal, C.J., Gupta, A., Barkam, S., Saraf, S., Das, S., Cho, H.J., Seal, S., 2017. Sci. Rep. 7 (1), 1324, 1324.
Niu, X., Cheng, N., Ruan, X., Du, D., Lin, Y., 2019. J. Electrochem. Soc. 167 (3), 037508.
Niu, X., Li, X., Lyu, Z., Pan, J., Ding, S., Ruan, X., Zhu, W., Du, D., Lin, Y., 2020. Chem. Commun. 56 (77), 11338–11353.
Nothling, M.D., Xiao, Z., Bhaskaran, A., Blyth, M.T., Bennett, C.W., Coote, M.L., Connal, L.A., 2019. ACS Catal. 9 (1), 168–187.
Ojani, R., Raoof, J.B., Zamani, S., 2012. Bioelectrochemistry 85, 44–49.

Oliveira, G.H.C., Ramos, L.M., de Paiva, R.K.C., Passos, S.T.A., Simões, M.M., Machado, F., Correa, J.R., Neto, B.A.D., 2021. Org. Biomol. Chem. 19 (7), 1514–1531.
Palecek, E., Bartosik, M., 2012. Chem. Rev. 112 (6), 3427–3481.
Palecek, E., Ostatna, V., Pechan, Z., 2014. Chem. Listy 108 (5), 490–499.
Panda, C., Ghosh, M., Panda, T., Banerjee, R., Sen Gupta, S., 2011. Chem. Commun. 47 (28), 8016–8018.
Parate, K., Karunakaran, C., Claussen, J.C., 2019. Sensor. Actuator. B Chem. 287, 165–172.
Parlak, O., Keene, S.T., Marais, A., Curto, V.F., Salleo, A., 2018. Sci. Adv. 4 (7), eaar2904.
Patra, C.R., 2016. Nanomedicine 11 (6), 569–572.
Pecht, I., Levitzki, A., Anbar, M., 1967. J. Am. Chem. Soc. 89 (7), 1587–1591.
Peng, R., Offenhäusser, A., Ermolenko, Y., Mourzina, Y., 2020. Sensor. Actuator. B Chem. 321.
Pereira da Silva Neves, M.M., González-García, M.B., Hernández-Santos, D., Fanjul-Bolado, P., 2018. Curr. Opin. Electrochem. 10, 107–111.
Perez Sirkin, Y.A., Tagliazucchi, M., Szleifer, I., 2020. Mater. Today Adv. 5.
Pesavento, M., Merli, D., Biesuz, R., Alberti, G., Marchetti, S., Milanese, C., 2021. Anal. Chim. Acta 1142, 201–210.
Qian, F., Zhang, W., Huang, D., Li, W., Wang, Q., Zhao, C., 2020. Phys. Chem. Chem. Phys. 22 (4), 2386–2398.
Qu, L., Yang, L., Ren, Y., Ren, X., Fan, D., Xu, K., Wang, H., Li, Y., Ju, H., Wei, Q., 2020. Sensor. Actuator. B Chem. 320, 128324.
Raba, J., Mottola, H.A., 1995. Crit. Rev. Anal. Chem. 25 (1), 1–42.
Radi, A.-E., Wahdan, T., El-Basiony, A., 2019. Curr. Anal. Chem. 15 (3), 219–239.
Raynal, M., Ballester, P., Vidal-Ferran, A., van Leeuwen, P., 2014a. Chem. Soc. Rev. 43 (5), 1660–1733.
Raynal, M., Ballester, P., Vidal-Ferran, A., van Leeuwen, P.W.N.M., 2014b. Chem. Soc. Rev. 43 (5), 1734–1787.
Rebelo, P., Costa-Rama, E., Seguro, I., Pacheco, J.G., Nouws, H.P.A., Cordeiro, M., Delerue-Matos, C., 2021. Biosens. Bioelectron. 172, 112719.
Rebilly, J.-N., Colasson, B., Bistri, O., Over, D., Reinaud, O., 2015. Chem. Soc. Rev. 44 (2), 467–489.
Reta, N., Michelmore, A., Saint, C.P., Prieto-Simon, B., Voelcker, N.H., 2019. ACS Sens. 4 (6), 1515–1523.
Reyes-De-Corcuera, J.I., Olstad, H.E., García-Torres, R., 2018. Ann. Rev. Food Sci. Technol. 9 (1), 293–322.
Romano-Rodríguez, A., Hernández-Ramírez, F., 2007. Microelectron. Eng. 84 (5–8), 789–792.
Roux, Y., Ricoux, R., Avenier, F., Mahy, J.P., 2015. Nat. Commun. 6.
Sanghavi, B.J., Mobin, S.M., Mathur, P., Lahiri, G.K., Srivastava, A.K., 2013. Biosens. Bioelectron. 39 (1), 124–132.
Santos, H., Martins, R.O., Soares, D.A., Chaves, A.R., 2020. Anal. Methods 12 (7), 894–911.
Savas, S., Altintas, Z., 2019. Materials 12 (13), 2189.
Scognamiglio, V., Antonacci, A., Lambreva, M.D., Litescu, S.C., Rea, G., 2015. Biosens. Bioelectron. 74, 1076–1086.
Scognamiglio, V., Pezzotti, G., Pezzotti, I., Cano, J., Buonasera, K., Giannini, D., Giardi, M.T., 2010. Microchim. Acta 170 (3), 215–225.
Sehit, E., Drzazgowska, J., Buchenau, D., Yesildag, C., Lensen, M., Altintas, Z., 2020. Biosens. Bioelectron. 165, 112432.
Sezgintürk, M.K., 2020. Chapter one - introduction to commercial biosensors. In: Sezgintürk, M.K. (Ed.), Commercial Biosensors and Their Applications. Elsevier, pp. 1–28.
Sgobbi, L.F., Machado, S.A.S., 2018. Biosens. Bioelectron. 100, 290–297.
Sgobbi, L.F., Zibordi-Besse, L., Rodrigues, B.V.M., Razzino, C.A., Da Silva, J.L.F., Machado, S.A.S., 2017. Catal. Sci. Technol. 7 (15), 3388–3398.
Sheet, D., Halder, P., Paine, T.K., 2013. Angew Chem. Int. Ed. Engl. 52 (50), 13314–13318.
Shim, J., Rivera, J.A., Bashir, R., 2013. Nanoscale 5 (22), 10887–10893.
Shin, H.Y., Park, T.J., Kim, M.I., 2015. J. Nanomater. 2015, 1–11.
Shu, J., Qiu, Z., Wei, Q., Zhuang, J., Tang, D., 2015a. Sci. Rep. 5, 15113.
Shu, J., Qiu, Z., Wei, Q., Zhuang, J., Tang, D., 2015b. Sci. Rep. 5 (1), 15113.
Silveira, C.M., Monteiro, T., Almeida, M.G., 2016. Biosensors 6 (4), 51.
Singh, S., 2019. Front. Chem. 7 (46), 1–10.
Singh, S., Singh, M., Mitra, K., Singh, R., Sen Gupta, S.K., Tiwari, I., Ray, B., 2017. Electrochim. Acta 258, 1435–1444.
Sode, K., Takahashi, Y., Ohta, S., Tsugawa, W., Yamazaki, T., 2001. Anal. Chim. Acta 435 (1), 151–156.
Soleymani, L., Li, F., 2017. ACS Sens. 2 (4), 458–467.
Song, Y., Qu, K., Zhao, C., Ren, J., Qu, X., 2010a. Adv. Mater. 22 (19), 2206–2210.
Song, Y., Wang, X., Zhao, C., Qu, K., Ren, J., Qu, X., 2010b. Chem. Eur J. 16 (12), 3617–3621.
Songa, E.A., Okonkwo, J.O., 2016. Talanta 155, 289–304.
Speltini, A., Scalabrini, A., Maraschi, F., Sturini, M., Profumo, A., 2017. Anal. Chim. Acta 974, 1–26.
Spetnagel, W.J., Klotz, I.M., 1976. J. Am. Chem. Soc. 98 (25), 8199–8204.
Sträter, N., Lipscomb, W.N., Klabunde, T., Krebs, B., 1996. Angew Chem. Int. Ed. Engl. 35 (18), 2024–2055.
Su, S., Lu, Z., Li, J., Hao, Q., Liu, W., Zhu, C., Shen, X., Shi, J., Wang, L., 2018. New J. Chem. 42 (9), 6750–6755.
Suh, J., 2001. Synlett 2001 (9), 1343–1363.
Suh, J., Hah, S.S., 1998. J. Am. Chem. Soc. 120 (39), 10088–10093.
Surya, S.G., Khatoon, S., Ait Lahcen, A., Nguyen, A.T.H., Dzantiev, B.B., Tarannum, N., Salama, K.N., 2020. RSC Adv. 10 (22), 12823–12832.
Tagliazucchi, M., Szleifer, I., 2015. Mater. Today 18 (3), 131–142.
Tello, A., Cao, R., Marchant, M.J., Gomez, H., 2016. Bioconjugate Chem. 27 (11), 2581–2591.
Tian, L., Qi, J., Oderinde, O., Yao, C., Song, W., Wang, Y., 2018a. Biosens. Bioelectron. 110, 110–117.
Tian, L., Qi, J., Qian, K., Oderinde, O., Cai, Y., Yao, C., Song, W., Wang, Y., 2018b. Sensor. Actuator. B Chem. 260, 676–684.
Tian, L., Qi, J., Qian, K., Oderinde, O., Liu, Q., Yao, C., Song, W., Wang, Y., 2018c. J. Electroanal. Chem. 812, 1–9.
Tian, L., Qian, K., Qi, J., Liu, Q., Yao, C., Song, W., Wang, Y., 2018d. Biosens. Bioelectron. 99, 564–570.
Tian, Y., Zhang, Z., Wen, L., Ma, J., Zhang, Y., Liu, W., Zhai, J., Jiang, L., 2013. Chem. Commun. 49 (91), 10679–10681.
Tu, J., Zhou, Z., Liu, Y., Li, T., Lu, S., Xiao, L., Xiao, P., Zhang, G., Sun, Z., 2021. RSC Adv. 11 (6), 3751–3758.
Ugalmugle, S., Swain, R., 2020. https://www.gminsights.com/industry-analysis/self-monitoring-blood-glucose-devices-market. (Accessed 22 February 2021).
Ugalmugle, S., Swain, R., 2021. https://www.gminsights.com/industry-analysis/biosensors-market. (Accessed 18 February 2021).
Uniyal, S., Sharma, R.K., 2018. Biosens. Bioelectron. 116, 37–50.
Upadhyay, S.S., Kalambate, P.K., Srivastava, A.K., 2019. J. Electroanal. Chem. 840, 305–312.
van Enter, B.J., von Hauff, E., 2018. Chem. Commun. 54 (40), 5032–5045.
Vasapollo, G., Sole, R.D., Mergola, L., Lazzoi, M.R., Scardino, A., Scorrano, S., Mele, G., 2011. Int. J. Mol. Sci. 12 (9), 5908–5945.
Verheyen, E., Schillemans, J.P., van Wijk, M., Demeniex, M.A., Hennink, W.E., van Nostrum, C.F., 2011. Biomaterials 32 (11), 3008–3020.
Vial, L., Dumy, P., 2009. New J. Chem. 33 (5), 939–946.
Waffo, A.F.T., Yesildag, C., Caserta, G., Katz, S., Zebger, I., Lensen, M.C., Wollenberger, U., Scheller, F.W., Altintas, Z., 2018. Sensor. Actuator. B Chem. 275, 163–173.
Wang, C., Liu, C., Luo, J., Tian, Y., Zhou, N., 2016. Anal. Chim. Acta 936, 75–82.
Wang, D., Song, X.L., Li, P., Gao, X.J.J., Gao, X.F., 2020a. J. Mater. Chem. B 8 (39), 9028–9034.
Wang, L., Miao, L., Yang, H., Yu, J., Xie, Y., Xu, L., Song, Y., 2017. Sensor. Actuator. B Chem. 253, 108–114.
Wang, P., Cao, L., Chen, Y., Wu, Y., Di, J., 2019. ACS Appl. Nano Mater. 2 (4), 2204–2211.
Wang, P., Wang, T., Hong, J., Yan, X., Liang, M., 2020b. Front. Bioeng. Biotechnol. 8 (15).
Wang, Q., Lei, J., Deng, S., Zhang, L., Ju, H., 2013. Chem. Commun. 49 (9), 916–918.
Wang, Q., Wei, H., Zhang, Z., Wang, E., Dong, S., 2018a. TrAC Trends Anal. Chem. (Reference Ed.) 105, 218–224.
Wang, S., Yang, L., He, G., Shi, B., Li, Y., Wu, H., Zhang, R., Nunes, S., Jiang, Z., 2020c. Chem. Soc. Rev. 49 (4), 1071–1089.
Wang, Z., Chen, Y., Dong, W., Zhou, J., Han, B., Jiao, J., Lan, L., Miao, P., Chen, Q., 2018b. Biosens. Bioelectron. 121, 257–264.
Wang, Z., Zhang, R., Yan, X., Fan, K., 2020d. Mater. Today 41, 81–119.
Wei, H., Wang, E., 2008. Anal. Chem. 80 (6), 2250–2254.
Wei, H., Wang, E., 2013. Chem. Soc. Rev. 42 (14), 6060–6093.
Wei, X., Guo, J., Lian, H., Sun, X., Liu, B., 2021a. Sensor. Actuator. B Chem. 329, 129205.
Wei, X., Guo, J., Lian, H., Sun, X., Liu, B., 2021b. Sensor. Actuator. B Chem. 329, 129205.
Weston, J., 2005. Chem. Rev. 105 (6), 2151–2174.
Wu, H., Tian, Q., Zheng, W., Jiang, Y., Xu, J., Li, X., Zhang, W., Qiu, F., 2019a. J. Solid State Electrochem. 23 (5), 1379–1388.
Wu, J., Lv, W., Yang, Q., Li, H., Li, F., 2021. Biosens. Bioelectron. 171, 112707.
Wu, J.J.X., Wang, X.Y., Wang, Q., Lou, Z.P., Li, S.R., Zhu, Y.Y., Qin, L., Wei, H., 2019b. Chem. Soc. Rev. 48 (4), 1004–1076.
Wulff, G., 2002. Chem. Rev. 102 (1), 1–28.
Xia, F., Zhang, X., Lou, X., Yuan, Q., 2018. Biosensors Based on Sandwich Assays. Springer Singapore, Singapore.
Xia, J., Cao, X., Wang, Z., Yang, M., Zhang, F., Lu, B., Li, F., Xia, L., Li, Y., Xia, Y., 2016. Sensor. Actuator. B Chem. 225, 305–311.
Xia, X., Li, H., Zhou, G., Ge, L., Li, F., 2020. Analyst 145 (20), 6617–6624.
Xiao, Y., Chen, S., Zhang, G., Li, Z., Xiao, H., Chen, C., He, C., Zhang, R., Yang, X., 2020. Analyst 145 (14), 4806–4814.
Xie, Z., Yang, M., Luo, L., Lv, Y., Song, K., Liu, S., Chen, D., Wang, J., 2020. Talanta 219, 121213.
Xu, C., Lin, Y., Wang, J., Wu, L., Wei, W., Ren, J., Qu, X., 2013a. Adv. Healthc. Mater. 2 (12), 1591–1599.
Xu, Q., Wu, M., Schneider, G., Houben, L., Malladi, S., Dekker, C., Yucelen, E., Dunin-Borkowski, R., Zandbergen, H., 2013b. ACS Nano 7 (2), 1566–1572.
Yan, X., Gu, Y., Li, C., Tang, L., Zheng, B., Li, Y., Zhang, Z., Yang, M., 2016. Biosens. Bioelectron. 77, 1032–1038.
Yanez-Sedeno, P., Campuzano, S., Pingarron, J.M., 2017. Anal. Chim. Acta 960, 1–17.
Yang, B., Fu, C., Li, J., Xu, G., 2018. Trac. Trends Anal. Chem. 105, 52–67.
Yang, B., Li, J., Deng, H., Zhang, L., 2016a. Crit. Rev. Anal. Chem. 46 (6), 469–481.
Yang, B., Li, J., Zhang, L., Xu, G., 2016b. Analyst 141 (20), 5822–5828.
Yang, L., Zhang, B., Xu, B., Zhao, F., Zeng, B., 2021. Talanta 224, 121845.
Yang, Y., Yan, W., Guo, C., Zhang, J., Yu, L., Zhang, G., Wang, X., Fang, G., Sun, D., 2020. Anal. Chim. Acta 1106, 1–21.
Yen, W.K., Huang, W.C., Hsu, J.P., 2020. Electrophoresis 41 (10–11), 802–810.
You, M., Yang, S., Tang, W., Zhang, F., He, P., 2018. Biosens. Bioelectron. 112, 72–78.
Yu, H., Zhang, W., Lv, S., Han, J., Xie, G., Chen, S., 2018. Chem. Commun. 54 (84), 11901–11904.
Zeng, H.H., Qiu, W.B., Zhang, L., Liang, R.P., Qiu, J.D., 2016. Anal. Chem. 88 (12), 6342–6348.

Zhang, D.-Y., Younis, M.R., Liu, H., Lei, S., Wan, Y., Qu, J., Lin, J., Huang, P., 2021. Biomaterials 271, 120706.
Zhang, G., Yu, Y., Guo, M., Lin, B., Zhang, L., 2019a. Sensor. Actuator. B Chem. 288, 564–570.
Zhang, L., Zhai, Y., Gao, N., Wen, D., Dong, S., 2008. Electrochem. Commun. 10 (10), 1524–1526.
Zhang, Q., Jiang, D., Xu, C., Ge, Y., Liu, X., Wei, Q., Huang, L., Ren, X., Wang, C., Wang, Y., 2020a. Sensor. Actuator. B Chem. 320.
Zhang, R., Chen, X., Sun, Z., Chen, S., Gao, J., Sun, Y., Li, H., 2019b. Anal. Chem. 91 (9), 6149–6154.
Zhang, T., Xing, Y., Song, Y., Gu, Y., Yan, X., Lu, N., Liu, H., Xu, Z., Xu, H., Zhang, Z., Yang, M., 2019c. Anal. Chem. 91 (16), 10589–10595.
Zhang, W., Hu, S., Yin, J.-J., He, W., Lu, W., Ma, M., Gu, N., Zhang, Y., 2016. J. Am. Chem. Soc. 138 (18), 5860–5865.
Zhang, X., Jiang, Y., Zhu, M., Xu, Y., Guo, Z., Shi, J., Han, E., Zou, X., Wang, D., 2020b. Chem. Eng. J. 383.
Zhang, X., Li, G., Chen, G., Wu, D., Zhou, X., Wu, Y., 2020c. Coord. Chem. Rev. 418.
Zhang, Z., Wang, X., Yang, X., 2011a. Analyst 136 (23), 4960–4965.
Zhang, Z., Zhang, X., Liu, B., Liu, J., 2017. J. Am. Chem. Soc. 139 (15), 5412–5419.
Zhang, Z., Zhu, H., Wang, X., Yang, X., 2011b. Microchim. Acta 174 (1), 183–189.
Zhao, J., Cai, X., Gao, W., Zhang, L., Zou, D., Zheng, Y., Li, Z., Chen, H., 2018. ACS Appl. Mater. Interfaces 10 (31), 26108–26117.
Zhao, S., Shi, Z., Guo, C.X., Li, C.M., 2019a. Chem. Commun. 55 (54), 7836–7839.
Zhao, S.F., Hu, F.X., Shi, Z.Z., Fu, J.J., Chen, Y., Dai, F.Y., Guo, C.X., Li, C.M., 2021. Nano Res. 14 (3), 879–886.
Zhao, W., Li, B., Xu, S., Huang, X., Luo, J., Zhu, Y., Liu, X., 2019b. J. Mater. Chem. B 7 (14), 2311–2319.
Zhao, Z., Pang, J., Liu, W., Lin, T., Ye, F., Zhao, S., 2019c. Mikrochim. Acta 186 (5), 295.
Zheng, J., Wang, B., Jin, Y., Weng, B., Chen, J., 2019. Microchim. Acta 186 (2), 95.
Zhou, Y., Liu, B., Yang, R., Liu, J., 2017. Bioconjugate Chem. 28 (12), 2903–2909.
Zhu, L., Cao, Y., Cao, G., 2014. Biosens. Bioelectron. 54, 258–261.
Zou, Z., Ma, X.Q., Zou, L., Shi, Z.Z., Sun, Q.Q., Liu, Q., Liang, T.T., Li, C.M., 2019. Nanoscale 11 (6), 2624–2630.